Studi su radiazione e clima alla Stazione di Osservazioni di Lampedusa

Alcide Giorgio di Sarra

ENEA, Laboratorio Analisi ed Osservazioni del Sistema Terra

Roma

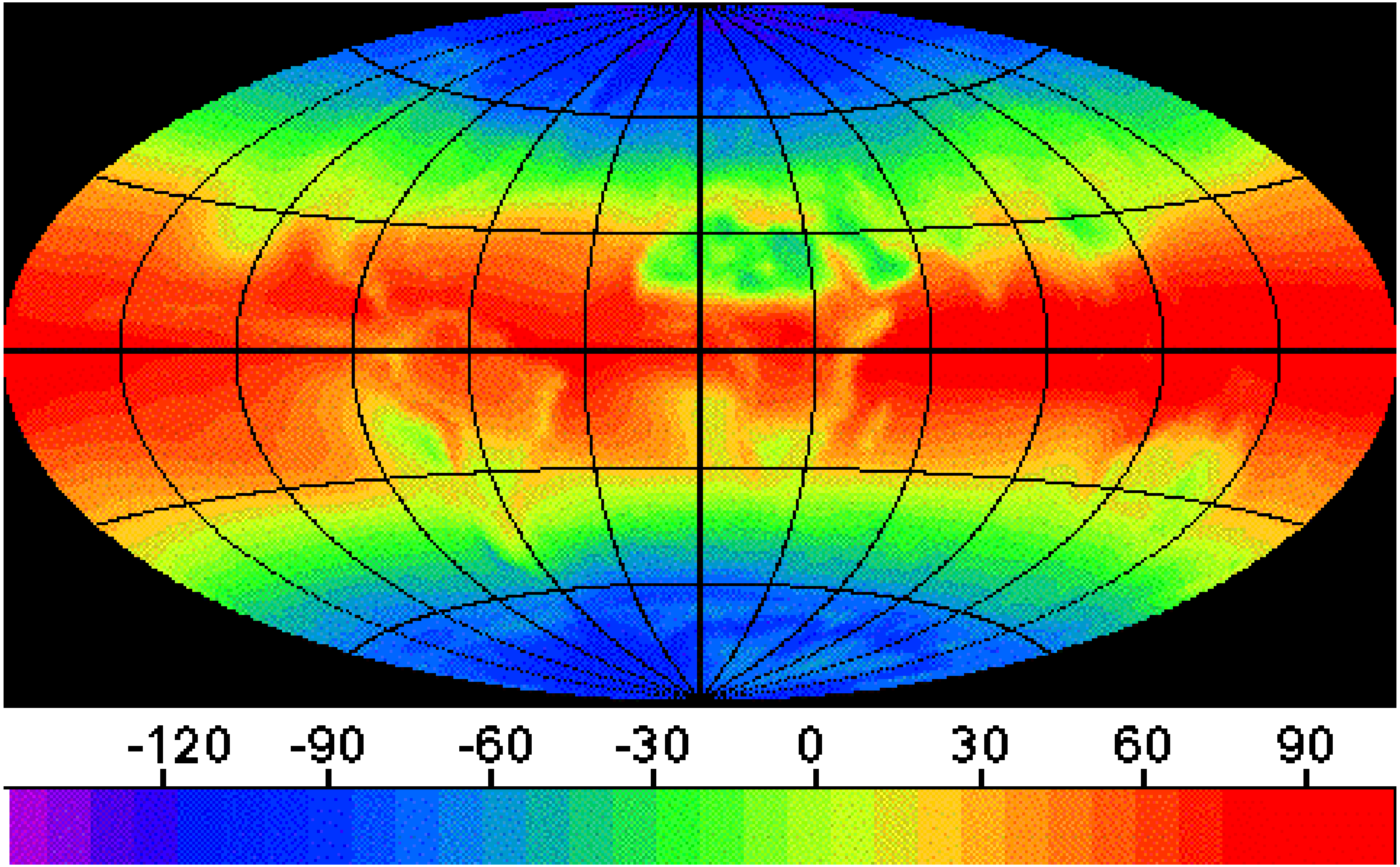

Net Radiation Budget [Wm^{-2}]

Mean from Feb. 1985 to Jan. 1989

(Thanks to MI-Hamburg)

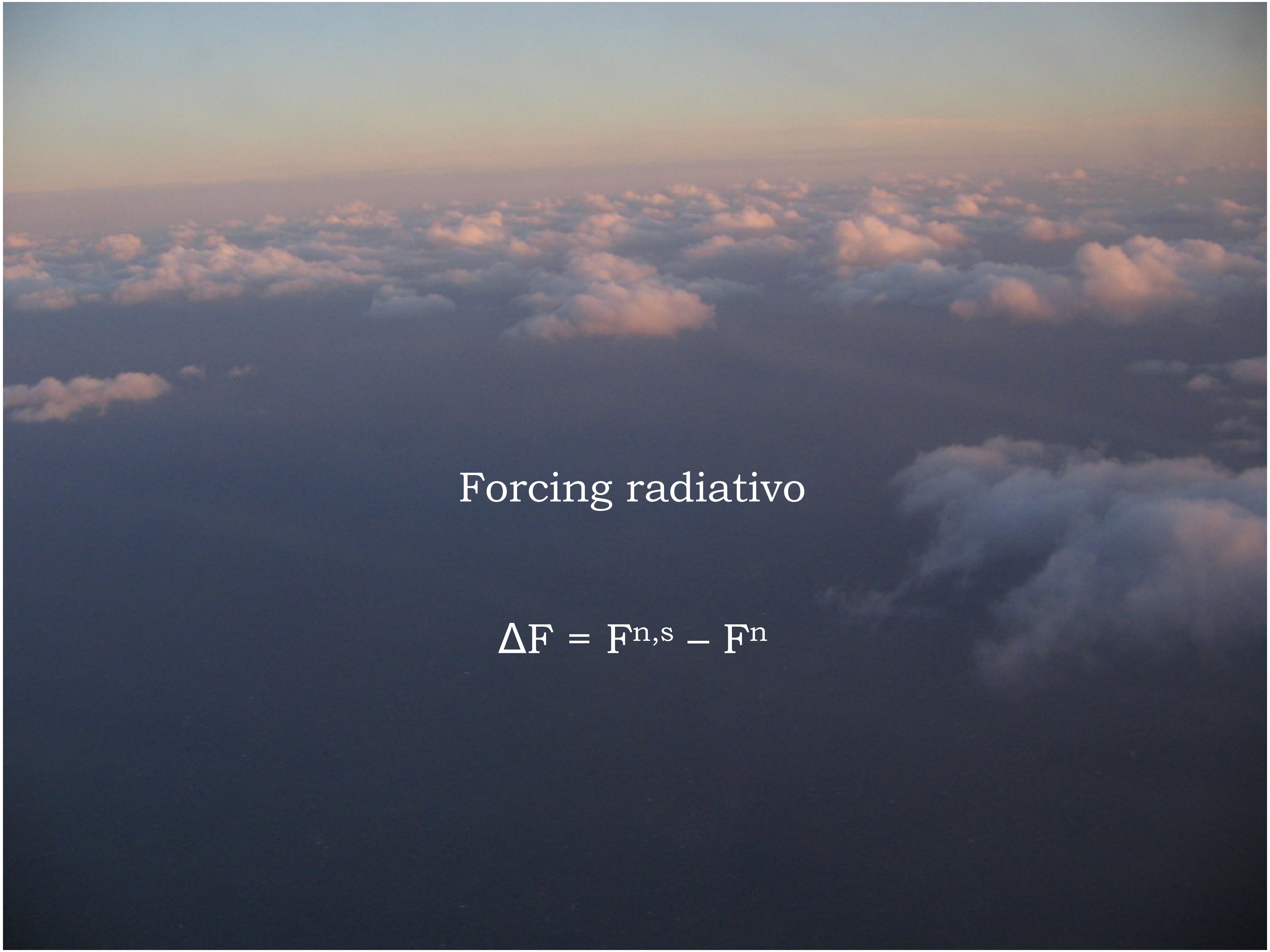
Forcing radiativo
$\Delta F = F^{n,s} - F^{n}$

IPCC, 2007

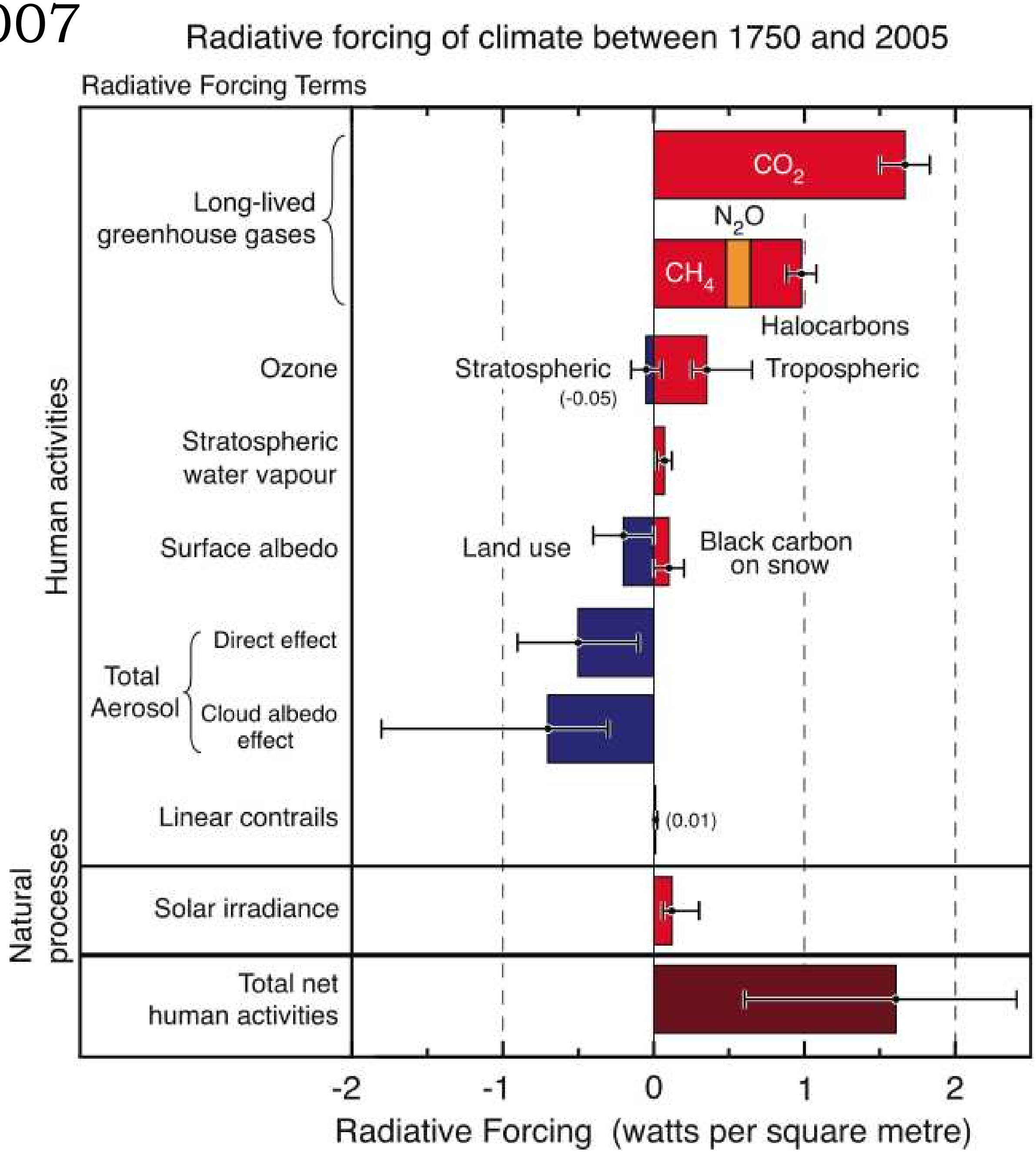

FAQ 2.1, Figure 2


ISS004E11850
35.5°N, 12.6°E
Picture ISS004E11850, courtesy of Earth Sciences and Image Analysis Laboratory
NASA Johnson Space Center (http://eol.jsc.nasa.gov)


http://www.lampedusa.enea.it


Stazione di Osservazioni Climatiche "Roberto Sarao"
ENEA
LAMPEDUSA
http://www.palermo.enea.it/lampedusa

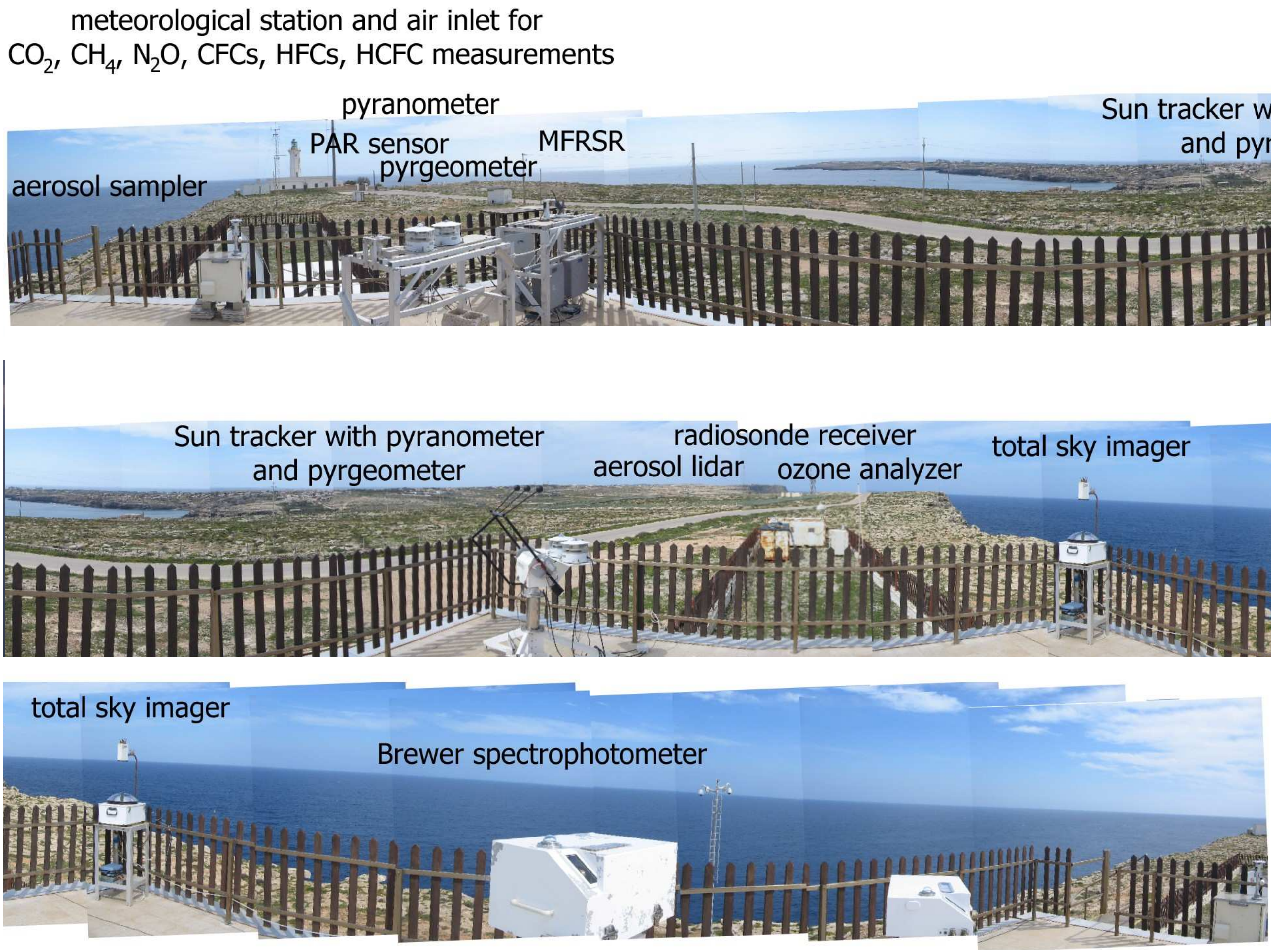
meteorological station and air inlet for
CO_2, CH_4, N_2O, CFCs, HFCs, HCFC measurements
pyranometer
PAR sensor
pyrgeometer
MFRSR
aerosol sampler
Sun tracker w
and pyr
Sun tracker with pyranometer
and pyrgeometer
radiosonde receiver
aerosol lidar
ozone analyzer
total sky imager
total sky imager
Brewer spectrophotometer

Instruments

- Meteorological station
- Non-dispersive Infra-red (NDIR) analyzer (atmospheric CO_2 mixing ratio)
- Gaschromatograph (atmospheric concentration of CH_4, N_2O, CFC-11 and CFC-12)
- Brewer MK III spectrophotometer (total ozone, spectral UV irradiance, aerosol optical depth)
- Precision Spectral Pyranometer/CMP21 (Shortwave irradiance)
- Precision IR radiometer/CGR4 (Longwave irradiance)
- Solar tracker with PSP and PIR (diffuse irradiance)
- CHP1 pyrheliometer (direct normal irradiance)
- Photosynthetic radiation radiometer
- Total sky imager (cloud cover)
- Actinic radiation spectrometer (photodissociation rates)
- Visible Multi Filter Rotating Shadowband Radiometer (MFRSR; aerosol optical depth at several wavelengths, diffuse-to-direct irradiance ratio, column water vapor)
- Ultraviolet Multi Filter Rotating Shadowband Radiometer (UV-MFRSR; aerosol optical depth, diffuse-to-direct irradiance ratio, total ozone)
- Aerosol lidar (University of Rome/ENEA; aerosol backscattering and depolarization) Cimel sun-photometer (aerosol optical properties, part of AERONET)
- PM10 filter sampler (chemical analyses at the University of Florence)
- CARAGA aerosol deposition sampler (LISA, France)
- PSAP (aerosol absorption, black carbon; ISPL, France)
- Radio-ozone sondes (ozone, pressure, temperature, humidity profiles)
- Ozone analyzer (Province of Agrigento)
- Raman lidar (University of Rome/ENEA; water vapour profiles)
- Microwave radiometer (water vapour/temperature profiles)
- IR camera (cloud altitude)

Weekly samples are collected for measurements of halogenated compounds carried out at Rome with a GC-MS (SF_6, HCFC-22, HCFC-134a, HCFC-142b, HCFC-141b, Halon-1301, CFC-11, CFC-12, CFC-113, CCl_4, $CHCl_3$)

Weekly samplings within the NOAA Cooperative air sampling network were started in October 2006 (CO_2, CH_4, CO, N_2O, H_2, ^{13}C, ^{18}O, SF_6)

WMO Global Atmosphere Watch
NOAA Cooperative Air Sampling Network
AERONET
MWRNet
Carboeurope

Measurement campaigns

PAUR II (1999), MEIDEX (2001), ENVISAT (2002), C-MARE (2004), LAUNCH (2005), AMP (2006), GAMARF(2008)

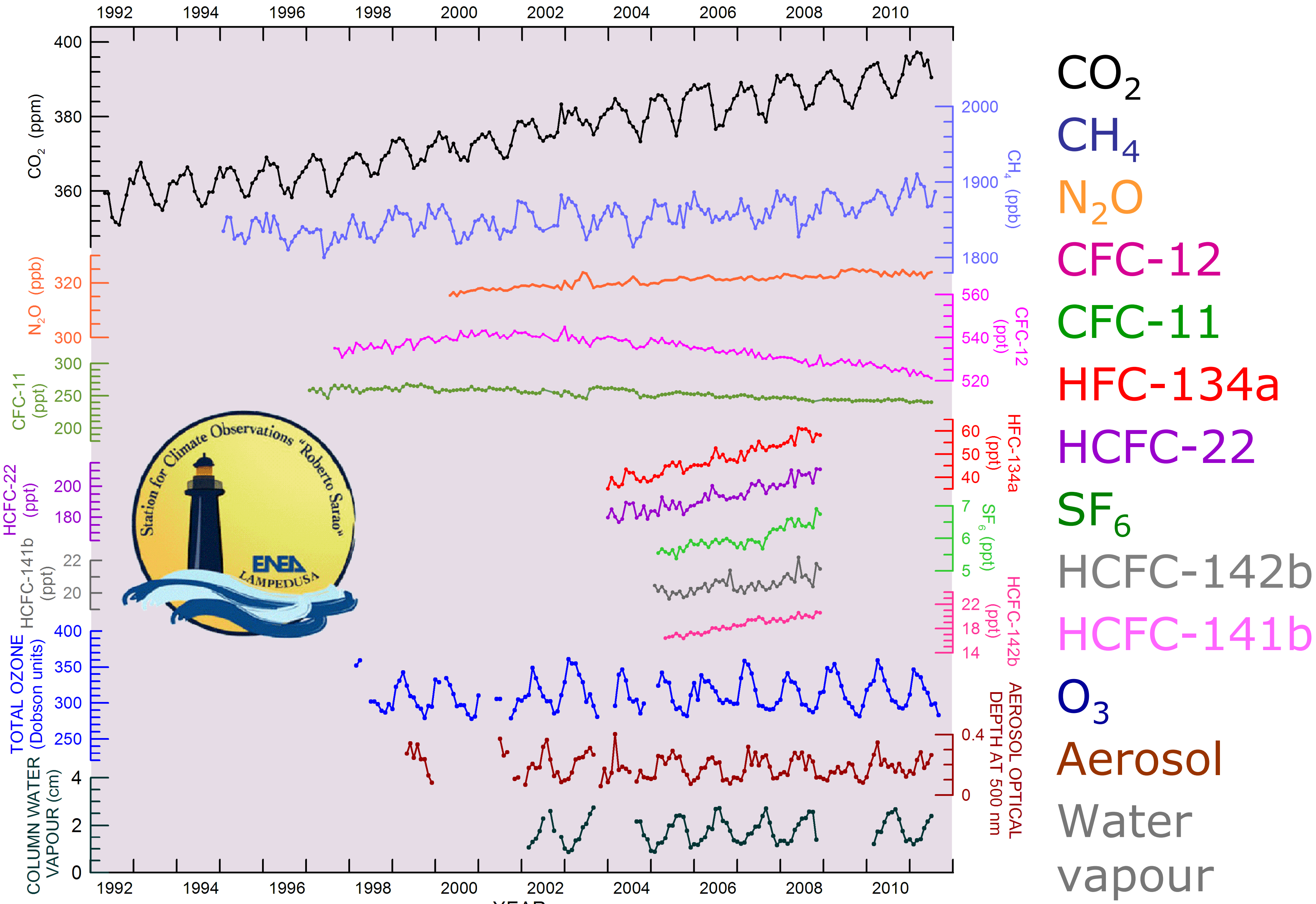

CO2
CH4
N2O
CFC-12
CFC-11
HFC-134a
HCFC-22
SF6
HCFC-142b
HCFC-141b
O3
Aerosol
Water vapour
YEAR
CO2 (ppm)
CH4 (ppb)
N2O (ppb)
CFC-12 (ppt)
CFC-11 (ppt)
HFC-134a (ppt)
HCFC-22 (ppt)
SF6 (ppt)
HCFC-141b (ppt)
HCFC-142b (ppt)
TOTAL OZONE (Dobson units)
AEROSOL OPTICAL DEPTH AT 500 nm
COLUMN WATER VAPOUR (cm)
Station for Climate Observations "Roberto Sarao"
ENEA
LAMPEDUSA

Surface shortwave irradiance I_{SW}

Eppley PSP and Kipp&Zone CMP21 pyranometers

I_{SW} (clouds, θ, τ, wv, A, …)

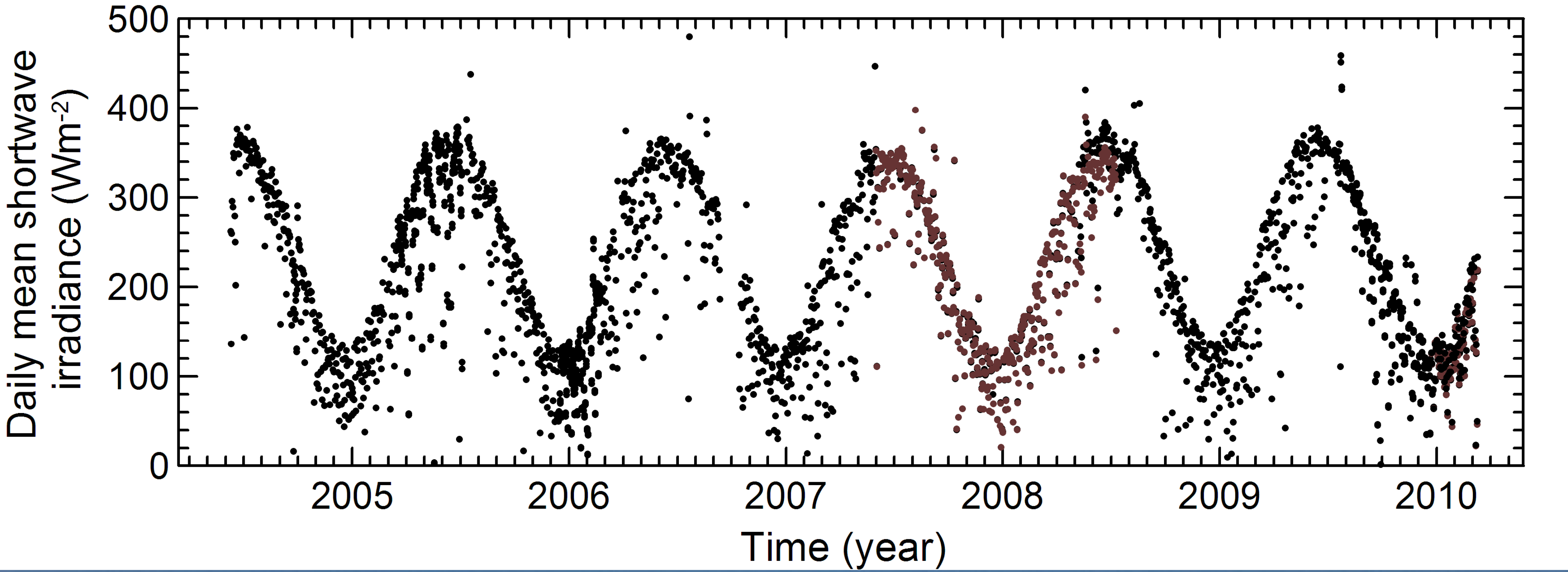

Solar irradiance 3%
IR irradiance 2%
Spectral UV irradiance 5%

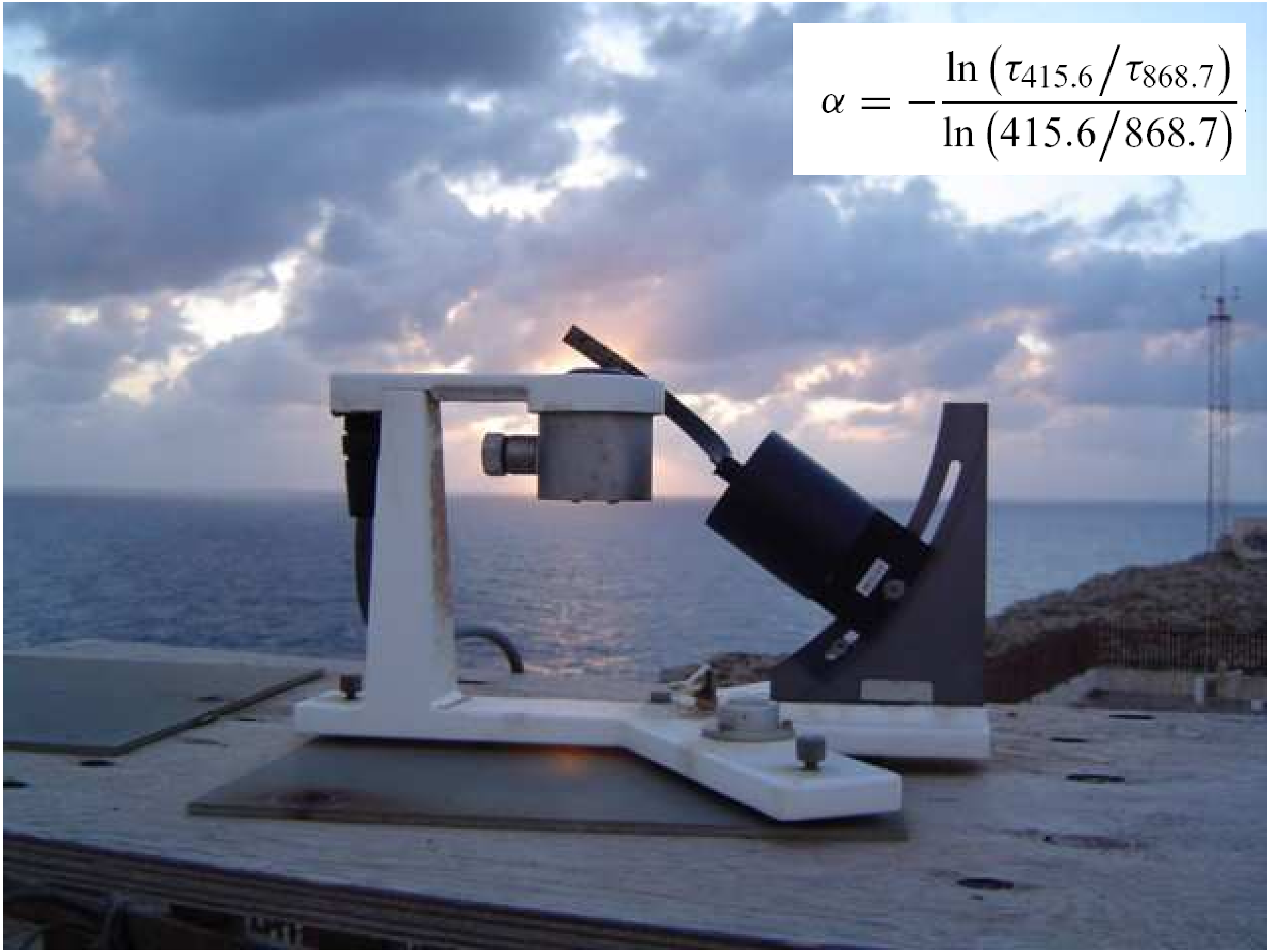

$$\alpha = -\frac{\ln\left(\tau_{415.6}/\tau_{868.7}\right)}{\ln\left(415.6/868.7\right)}$$

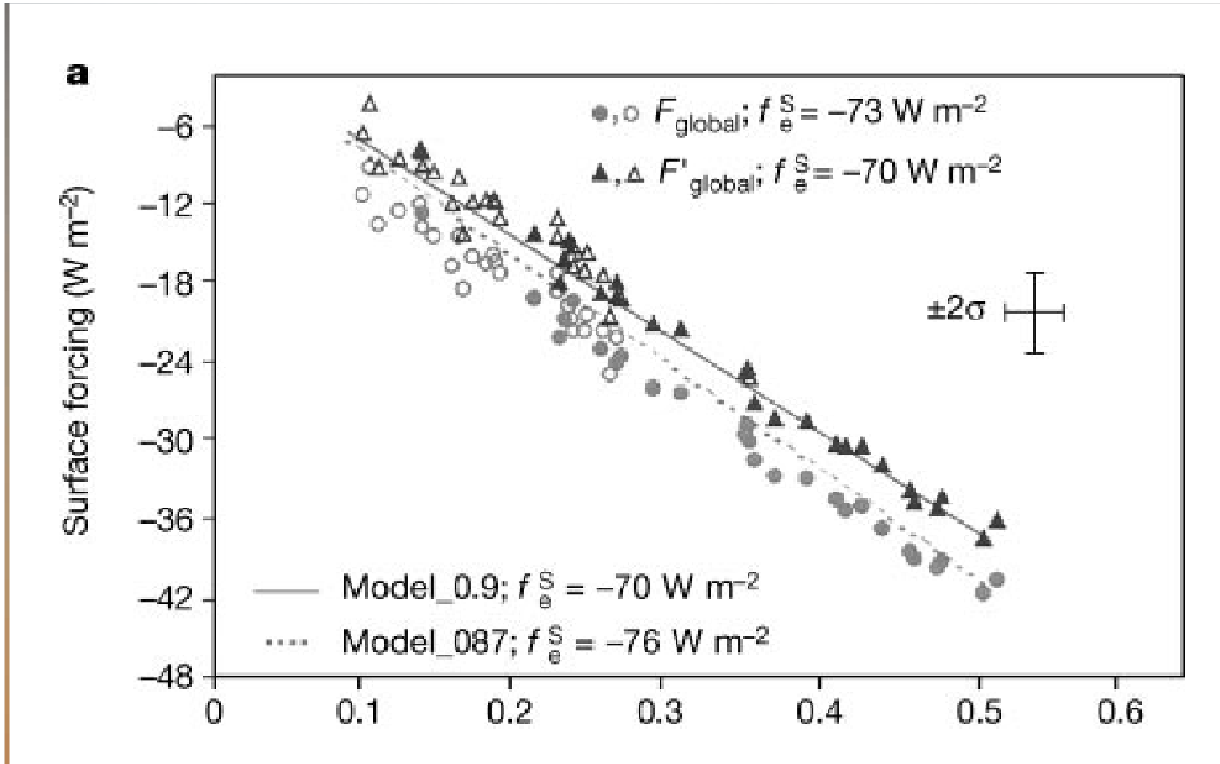

Satheesh and Ramanathan, 2000

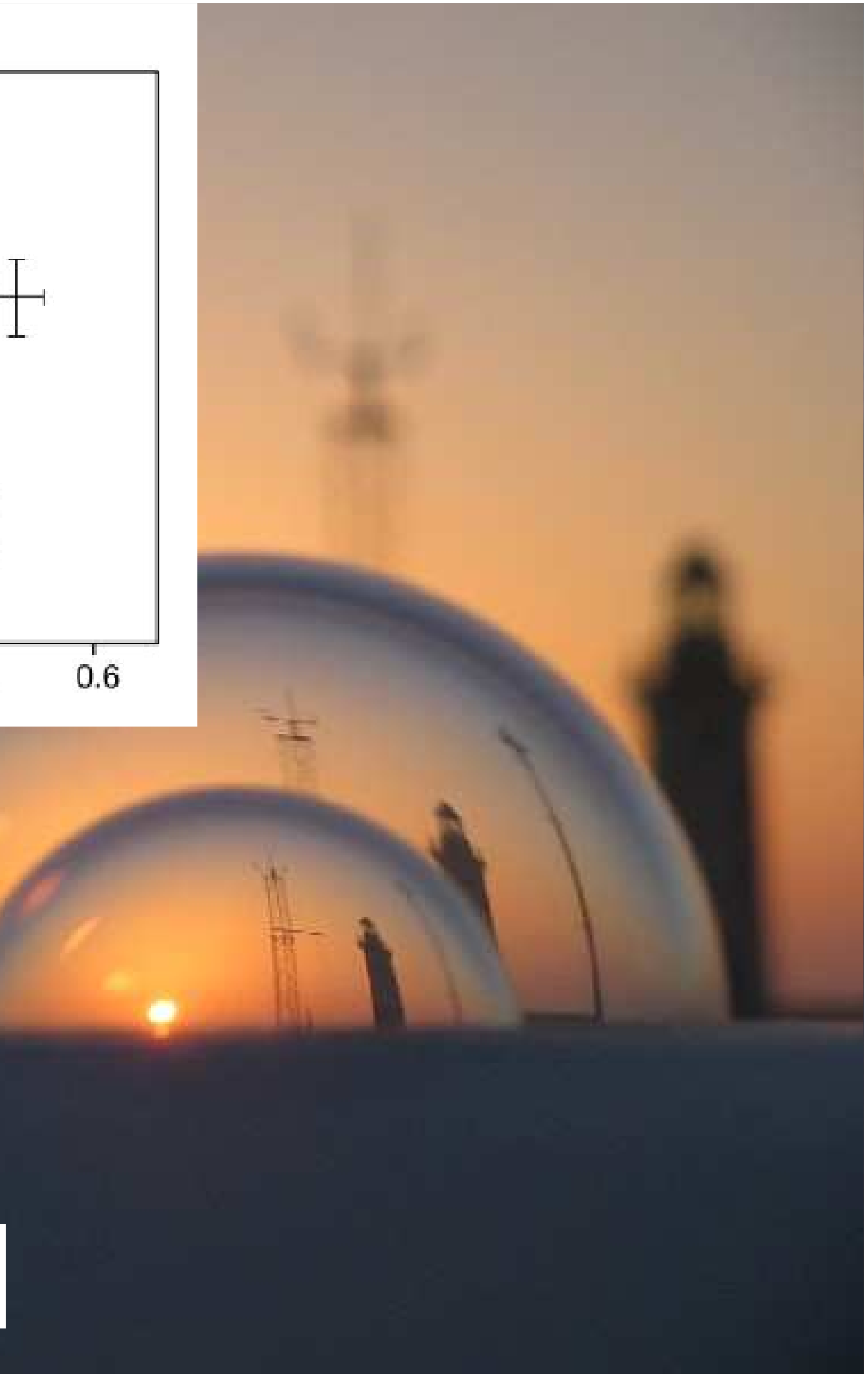

Stima del forcing

$$F_{net} = (1 - A) I_m$$

$$RF = F_{net} - F_{net}^{p} = (1 - A)\left(I_m - I_p\right)$$

$$FE(\theta) = dF_{net}(\theta)/d\tau(\theta)$$

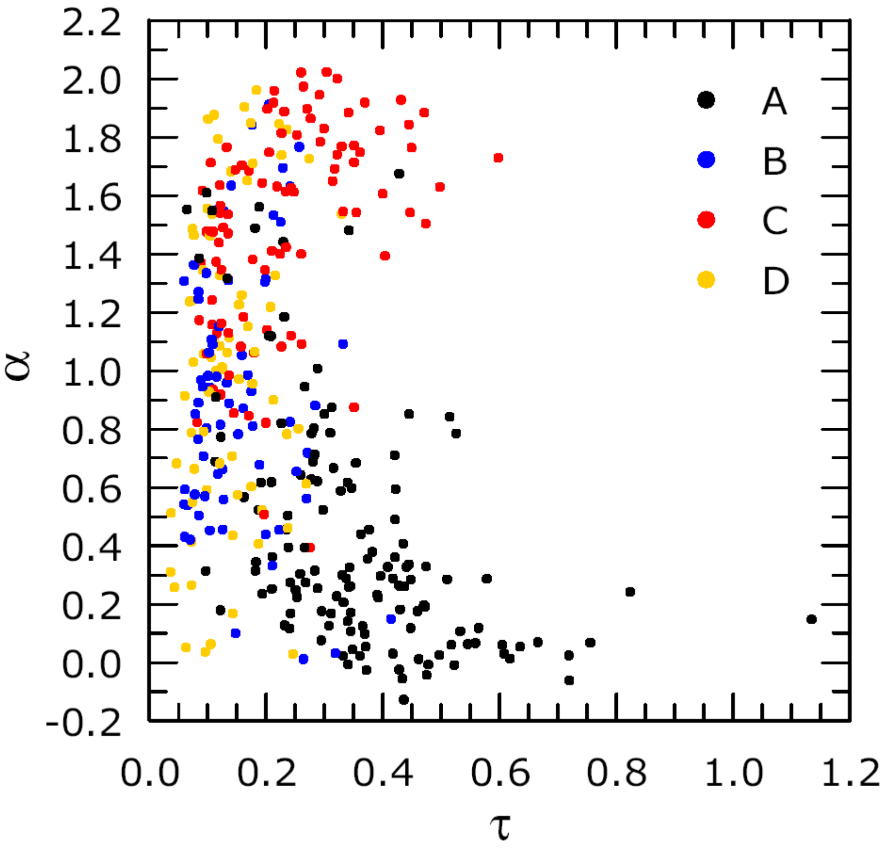
A
B
C
D
α
τ
2.2
2.0
1.8
1.6
1.4
1.2
1.0
0.8
0.6
0.4
0.2
0.0
-0.2
0.0
0.2
0.4
0.6
0.8
1.0
1.2

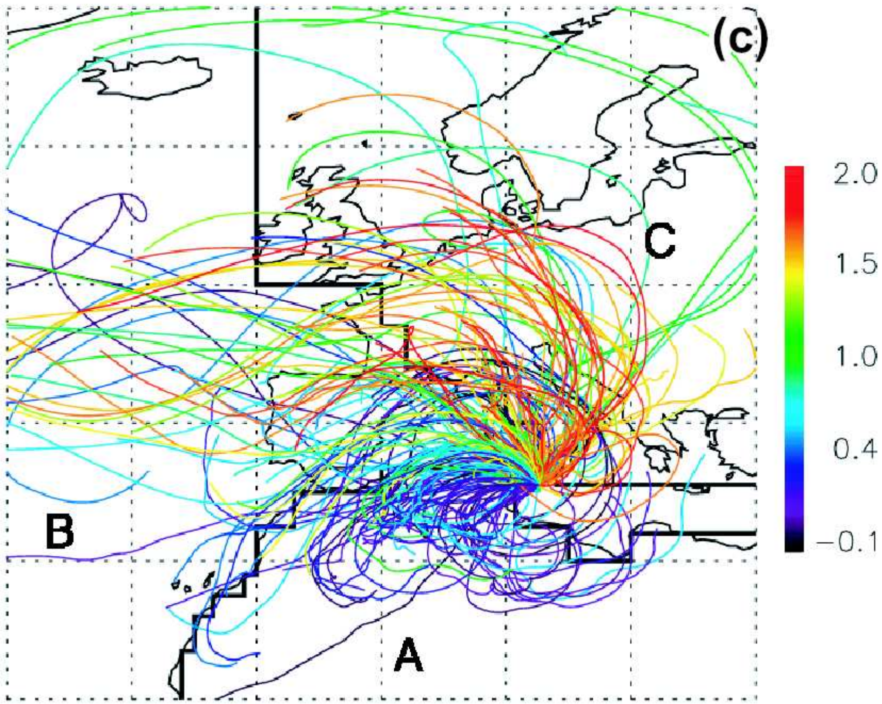
(c)
C
B
A
2.0
1.5
1.0
0.4
−0.1

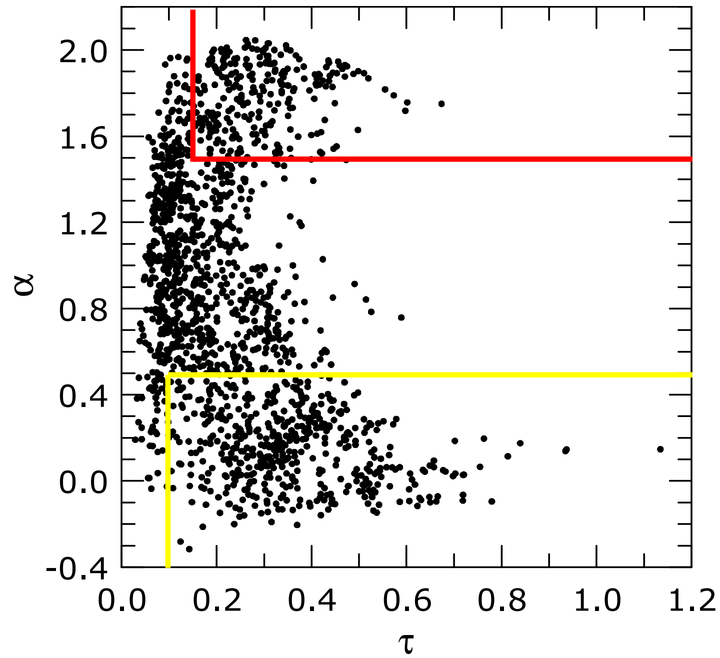
α
τ
2.0
1.6
1.2
0.8
0.4
0.0
-0.4
0.0
0.2
0.4
0.6
0.8
1.0
1.2


CLOUDS AND THE EARTH'S RADIANT ENERGY SYSTEM
CERES
PSP
Cimel
PIR
MFRSR

Surface aerosol FE: aerosol types

2004-2007

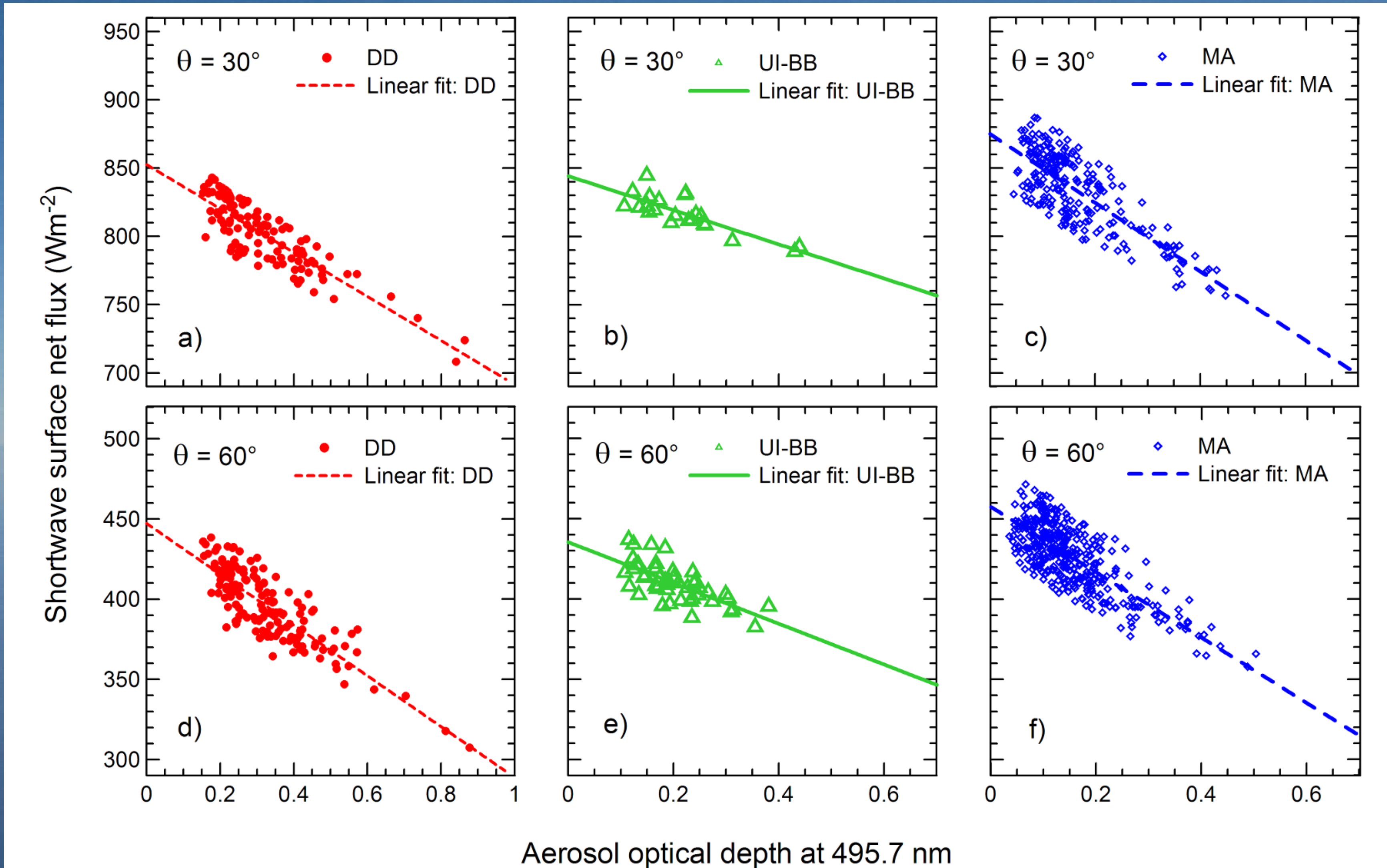

Di Biagio et al., *J. Geophys. Res.*, 2009

Aerosol FE at the top of the atmosphere

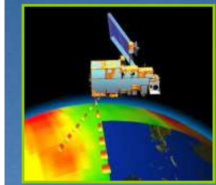

$$FE_{TOA} = \frac{d\left[-I_{SW,TOA}\right]}{d\tau}$$

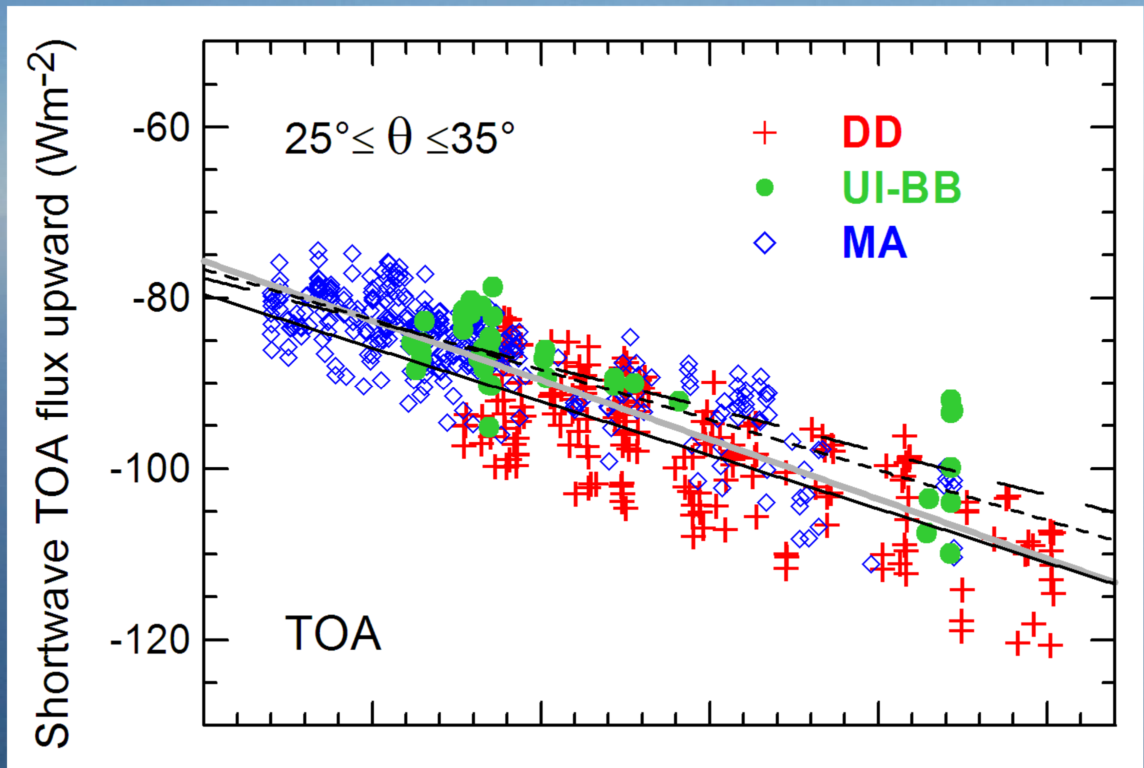

Di Biagio et al., 2010

Daily mean aerosol forcing efficiency

FE_S and FE_{TOA} at different θ → integrated to obtain the daily FE

	FE_d at the equinox (Wm^{-2})		
	TOA	**Surface**	**Atm**
DD	-45.5 ± 5.4	-68.9 ± 4.0	23.4 ± 6.7
UI-BB	-19.2 ± 3.3	-59.0 ± 4.3	39.8 ± 5.4
MA	-36.2 ± 1.7	-94.9 ± 5.1	58.7 ± 5.4

	FE_d at the summer solstice (Wm^{-2})		
	TOA	**Surface**	**Atm**
DD	-47.3 ± 5.6	-87.5 ± 5.0	40.2 ± 7.5
UI-BB	-23.3 ± 4.1	-75.6 ± 7.9	52.3 ± 8.9
MA	-44.2 ± 2.1	-120.5 ± 6.5	76.3 ± 6.8

The atmospheric forcing is ~30-50% of the surface forcing for DD, ~70% for UI-BB, and ~60% for MA.

Daily mean aerosol radiative forcing

The **daily mean radiative forcing** (**RF_d**) at TOA and at the surface are largest for DD due to the high value of both FE_d and average τ.

The atmospheric RF_d, conversely, is approximately independent of the aerosol type.

$$\boxed{RF_d = FE_d \cdot \tau}$$

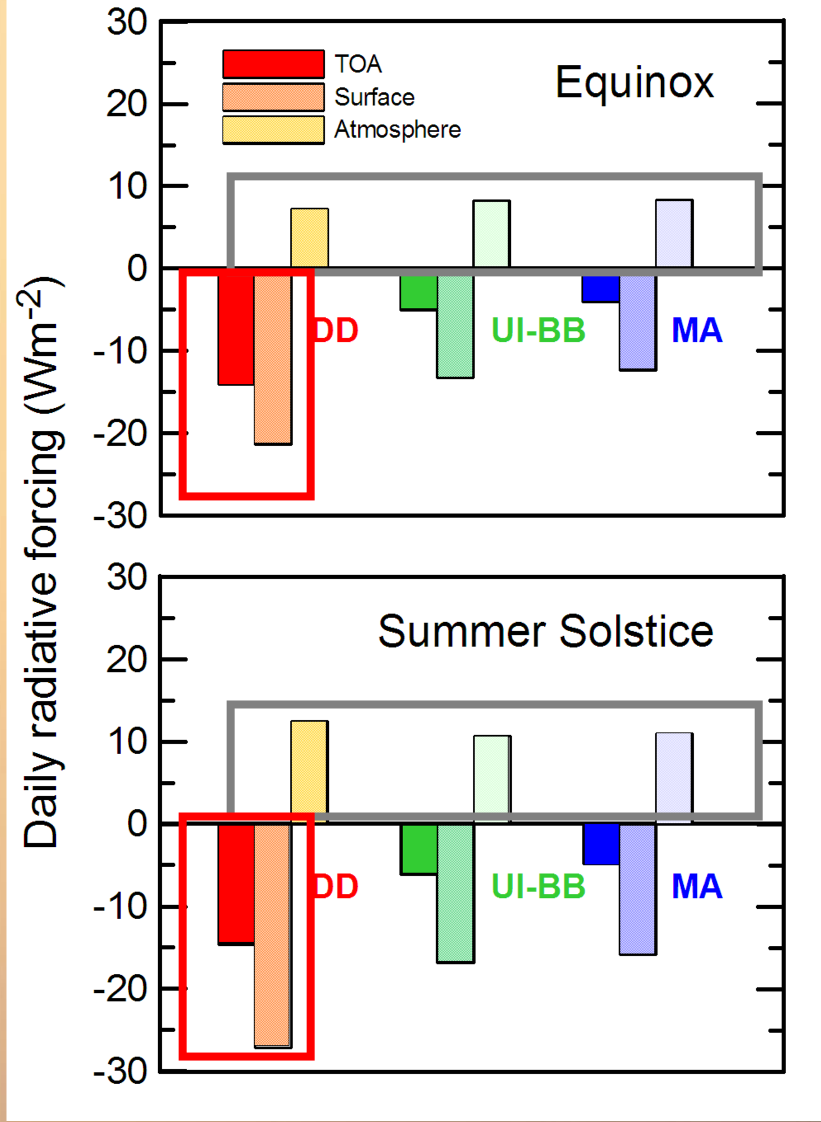

Derivazione dell'albedo di scattering singolo a 415.6 e 868.7 nm

$$k_{ext} = k_{sca} + k_{ass}$$

$$SSA = \frac{k_{sca}}{k_{ext}}$$

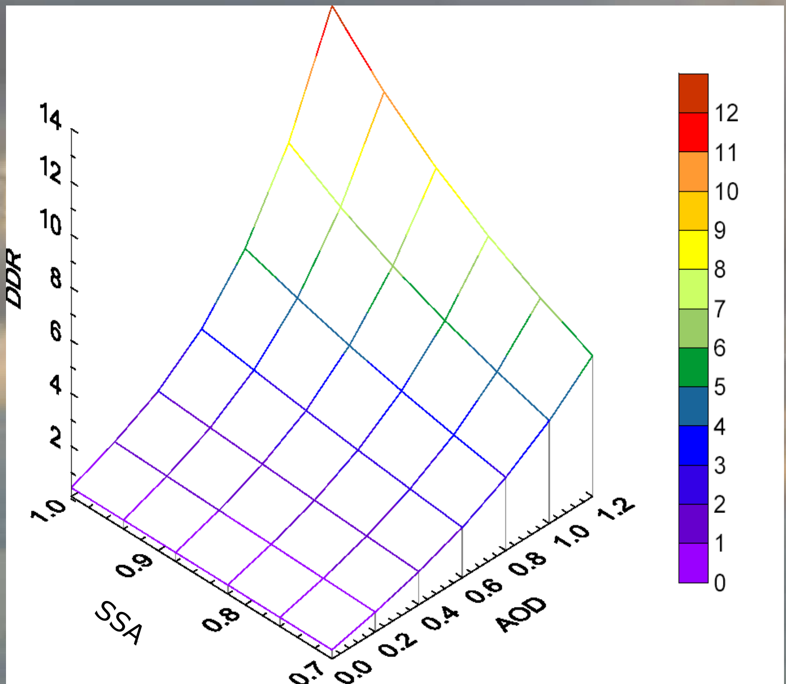

Aerosol desertico, 415.6 nm

Parametri forniti al modello LibRadTran:
SZA=60°
Profili verticali climatologici di pressione, temperatura, ozono, aerosol;
O_3 totale = 300 DU.

Si costruiscono funzioni per:
AOD(λ) tra 0 e 1.2;
SSA(λ) tra 0.7 e 1.0;
g(λ) dalla letteratura.

Da DDR(λ), AOD(λ), α misurati

SSA(λ)

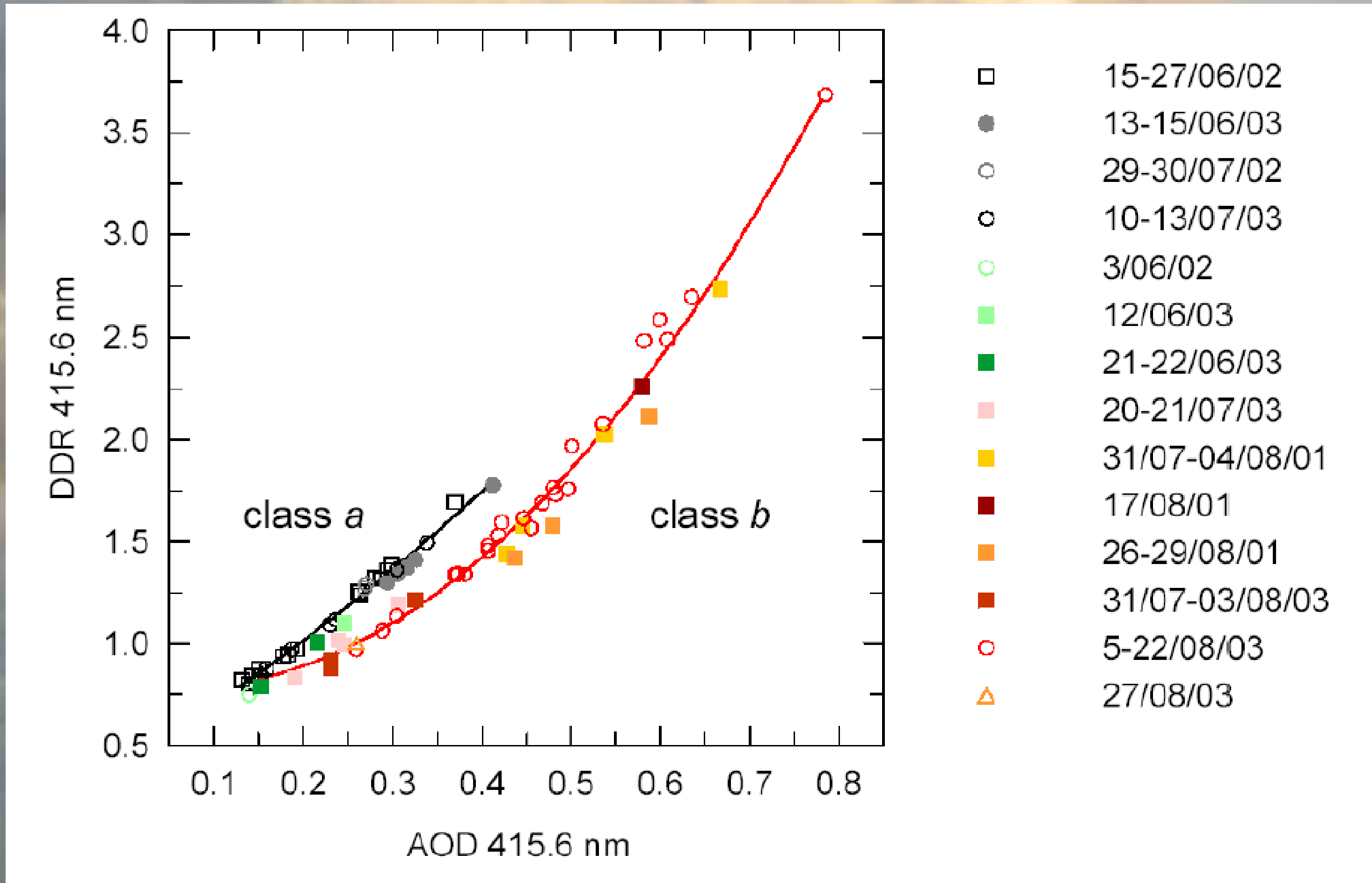

Meloni et al., 2006

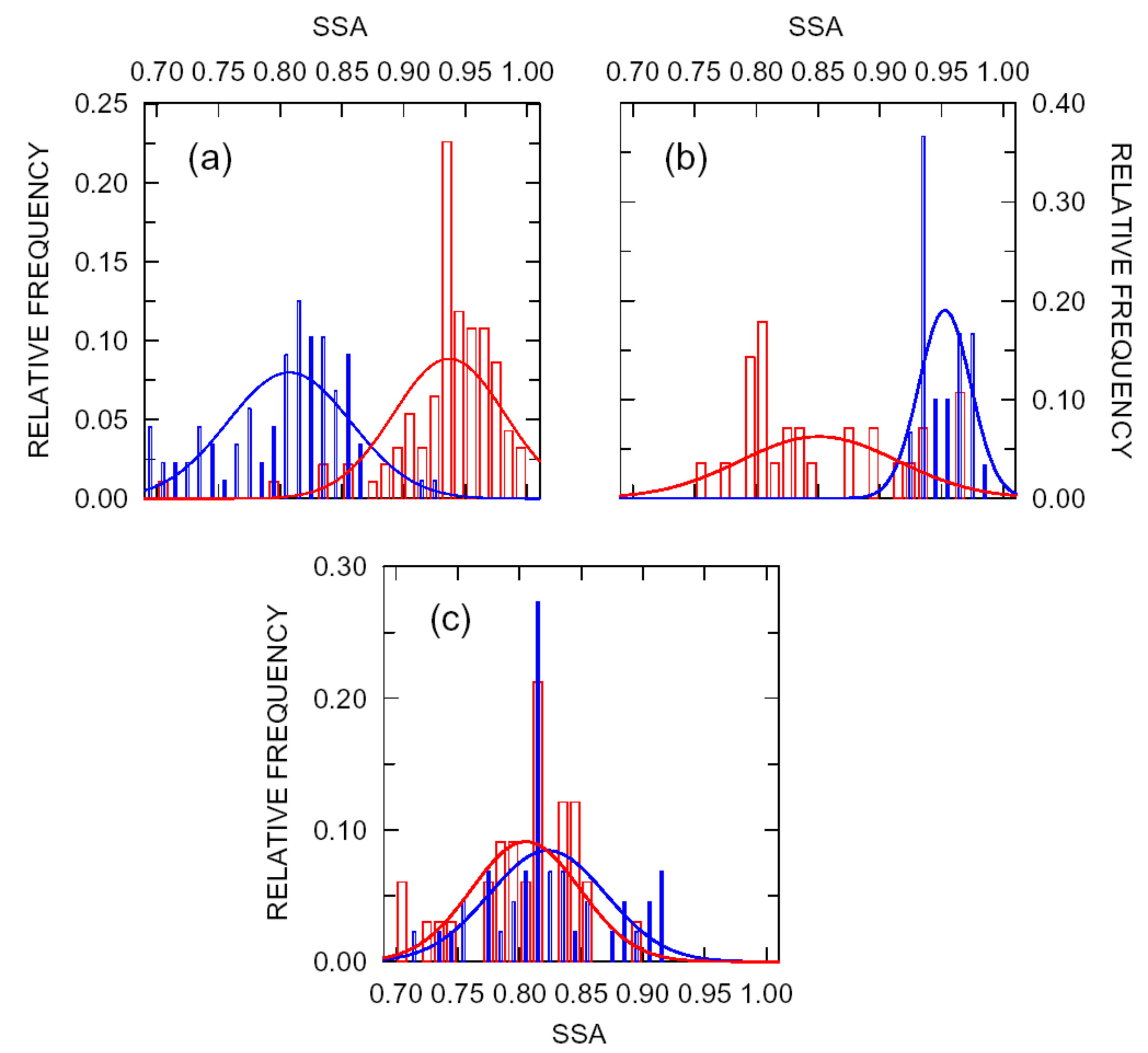

Meloni et al., 2006

Surface

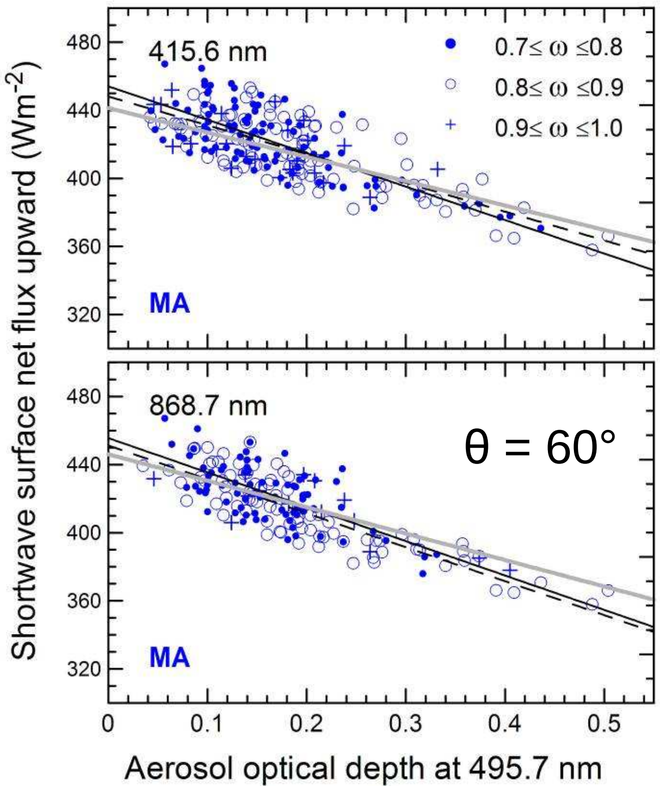

TOA (top of atmosphere)

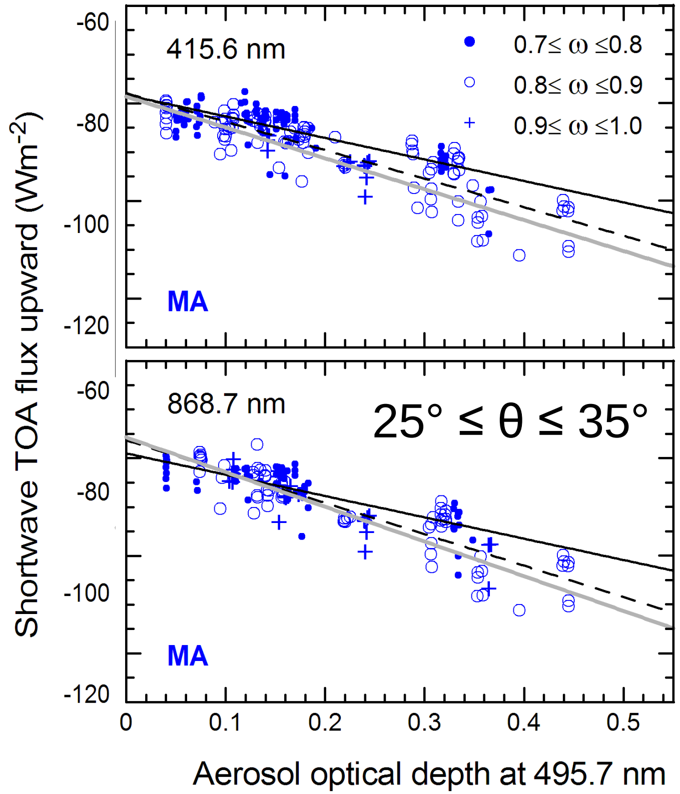

Di Biagio et al., 2009 and 2010

FE for DD and MA

- 0.7 ≤ ω < 0.8
- 0.8 ≤ ω < 0.9
- 0.9 ≤ ω ≤ 1.0

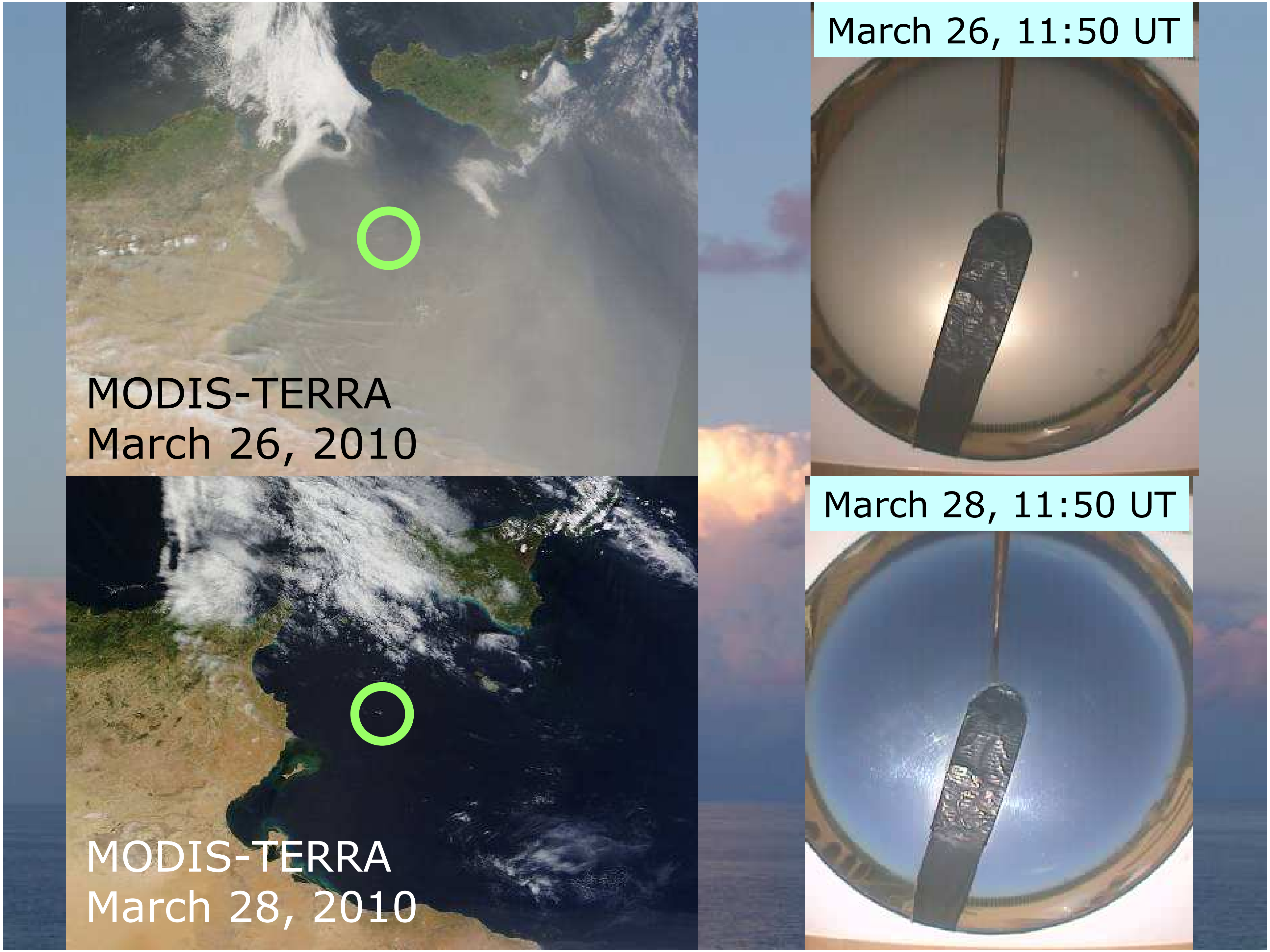
MODIS-TERRA
March 26, 2010
March 26, 11:50 UT
MODIS-TERRA
March 28, 2010
March 28, 11:50 UT

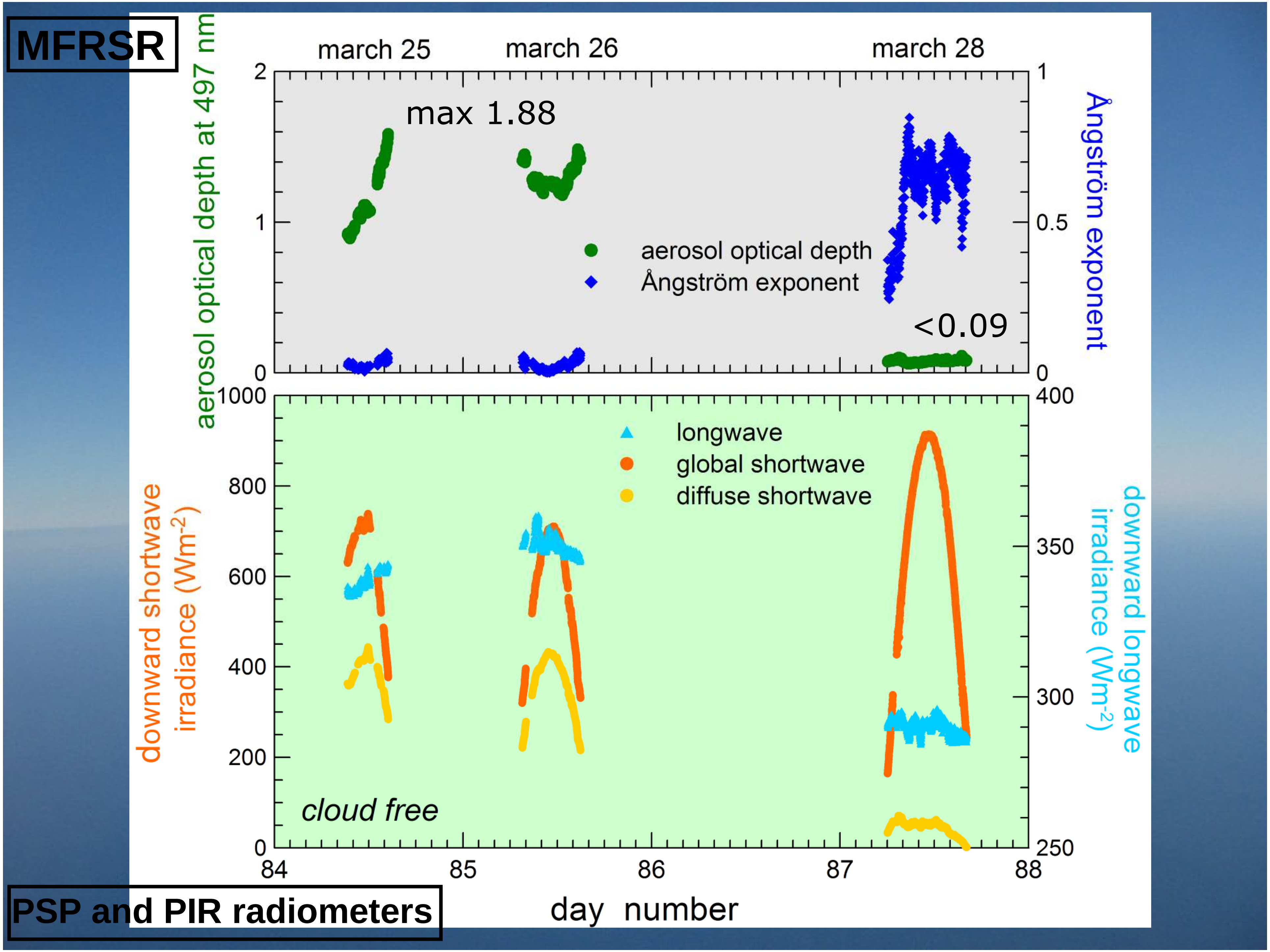
MFRSR
march 25
march 26
march 28
max 1.88
aerosol optical depth
Ångström exponent
<0.09
aerosol optical depth at 497 nm
Ångström exponent
longwave
global shortwave
diffuse shortwave
downward shortwave irradiance (Wm-2)
downward longwave irradiance (Wm-2)
cloud free
day number
PSP and PIR radiometers

instantaneous, at 35° solar zenith angle, LW, SW, and total forcing, for 26 March, 2010.

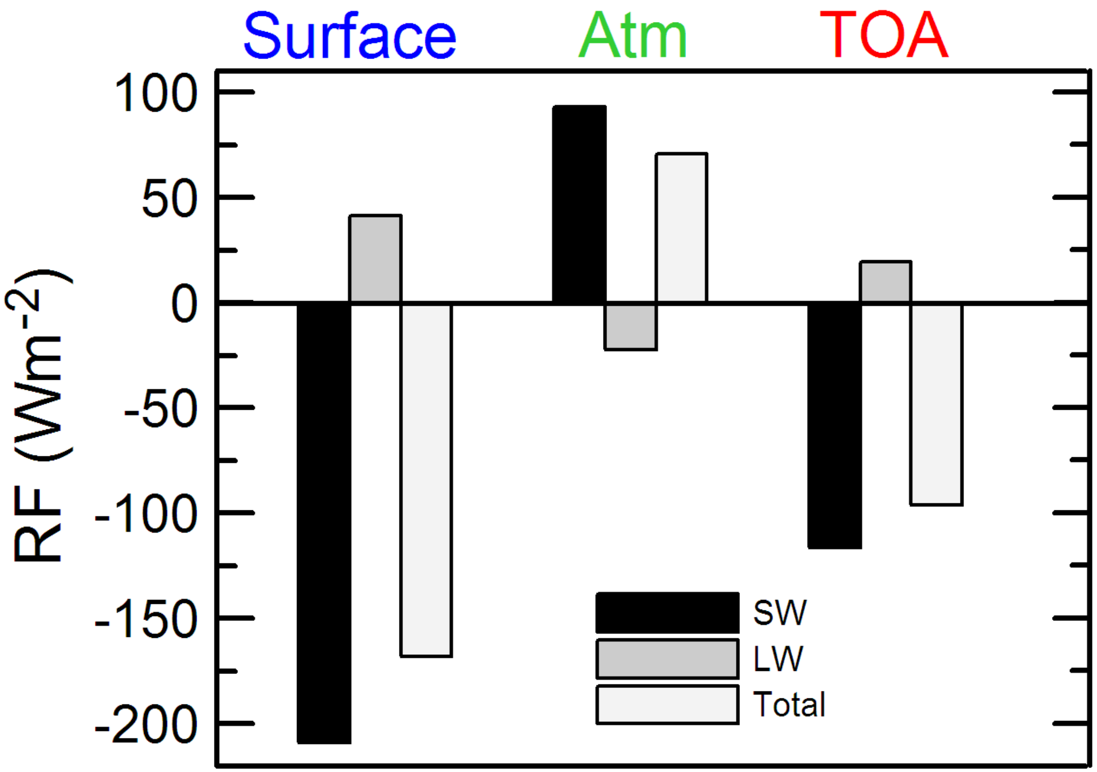

On a **daily** basis: surface LW RF is about 50% of the SW
TOA LW RF is about 40% of the SW
a bout 75% of the SW atmospheric RF is compensated by the LW RF

di Sarra et al., 2011

IPCC, 2007

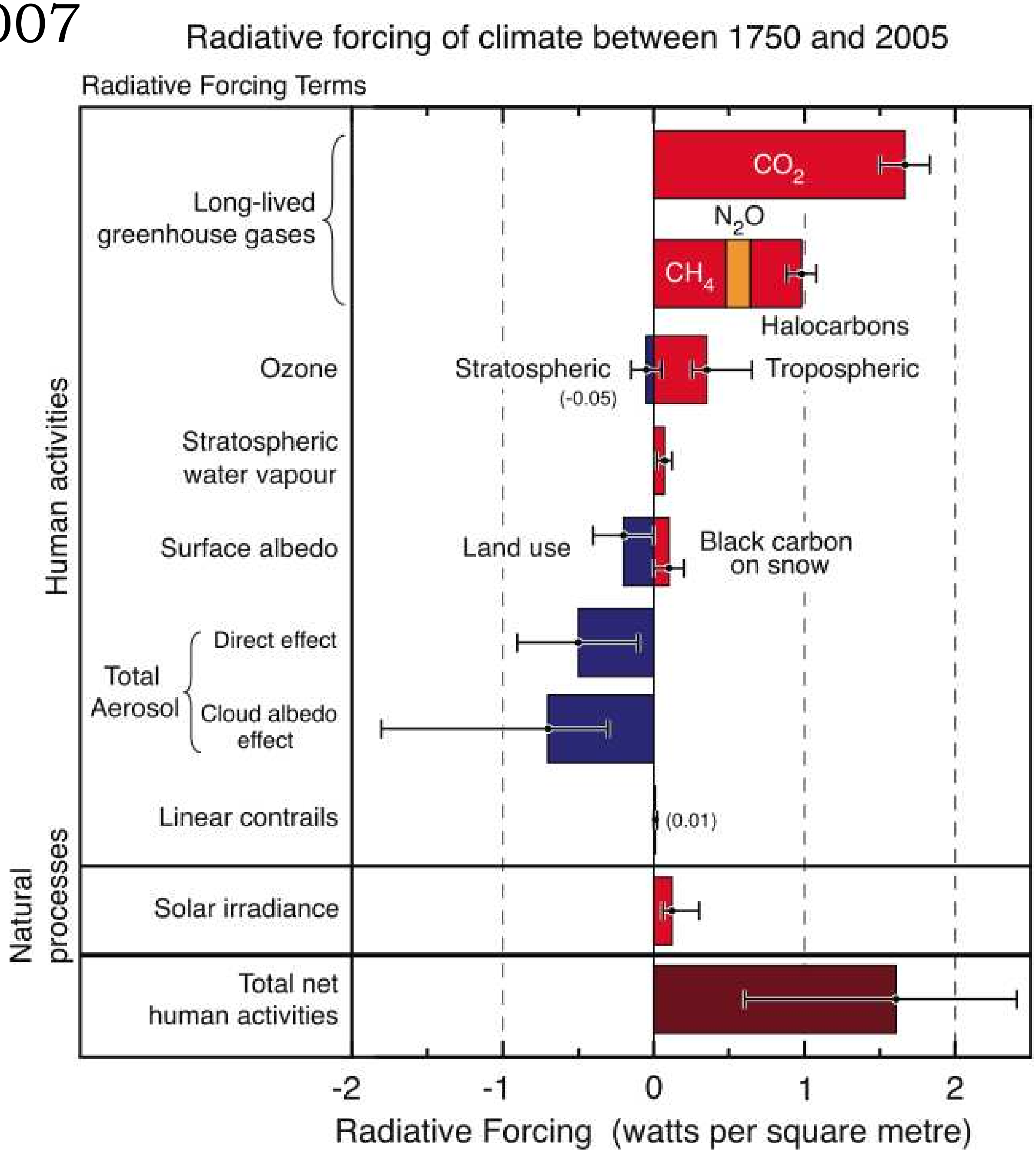

FAQ 2.1, Figure 2


Clouds
IR effects
UV-air quality
Stazione di Osservazioni Climatiche "Roberto Sarao"
ENEA
LAMPEDUSA
Grazie

Fabrizio Anello, Carlo Bommarito, Lorenzo De Silvestri, Claudia Di Biagio, Tatiana Di Iorio, Daniela Meloni, Francesco Monteleone, Giandomenico Pace, Salvatore Piacentino, Damiano Sferlazzo

http://www.lampedusa.enea.it

$$O_3 + h\nu \rightarrow O(^1D) + O_2 \quad \lambda < 320\,nm$$

$$O(^1D) + H_2O \rightarrow 2OH$$

$$AB + h\nu \rightarrow A + B$$

$$\frac{dn_A}{dt} = \frac{dn_B}{dt} = -j_{AB}\,n_{AB}$$

$$j_{AB} = \int_{\lambda_2}^{\lambda_1} \phi_{AB}(\lambda,T)\,\sigma_{AB}(\lambda,T)\,F_\lambda\,d\lambda$$

n_A, n_B, n_{AB}	densità numeriche
σ_{AB}	sezione d'urto
ϕ_{AB}	efficienza quantica
F_λ	flusso attinico

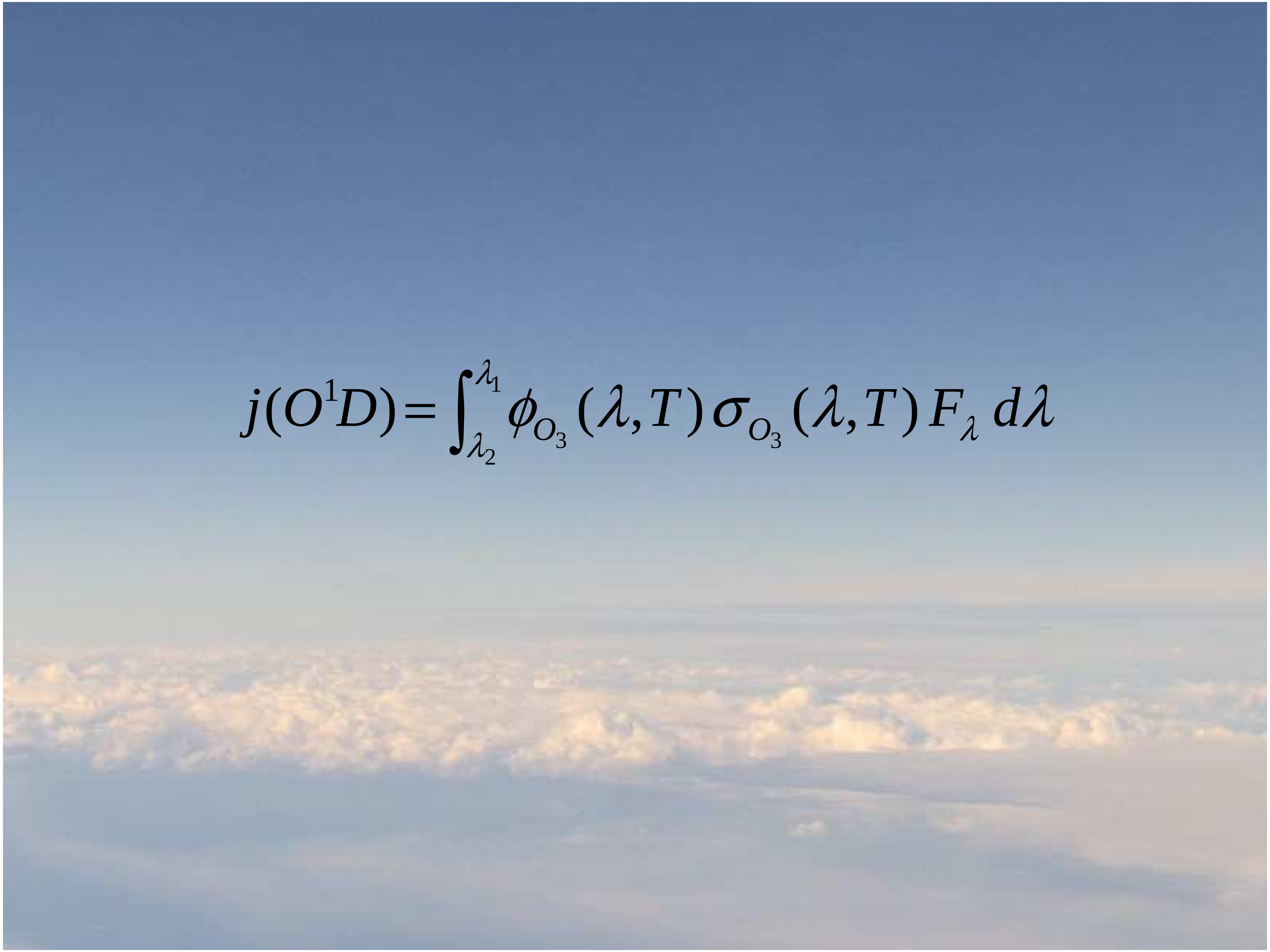

$$j(O^1D) = \int_{\lambda_2}^{\lambda_1} \phi_{O_3}(\lambda, T)\, \sigma_{O_3}(\lambda, T)\, F_\lambda \, d\lambda$$

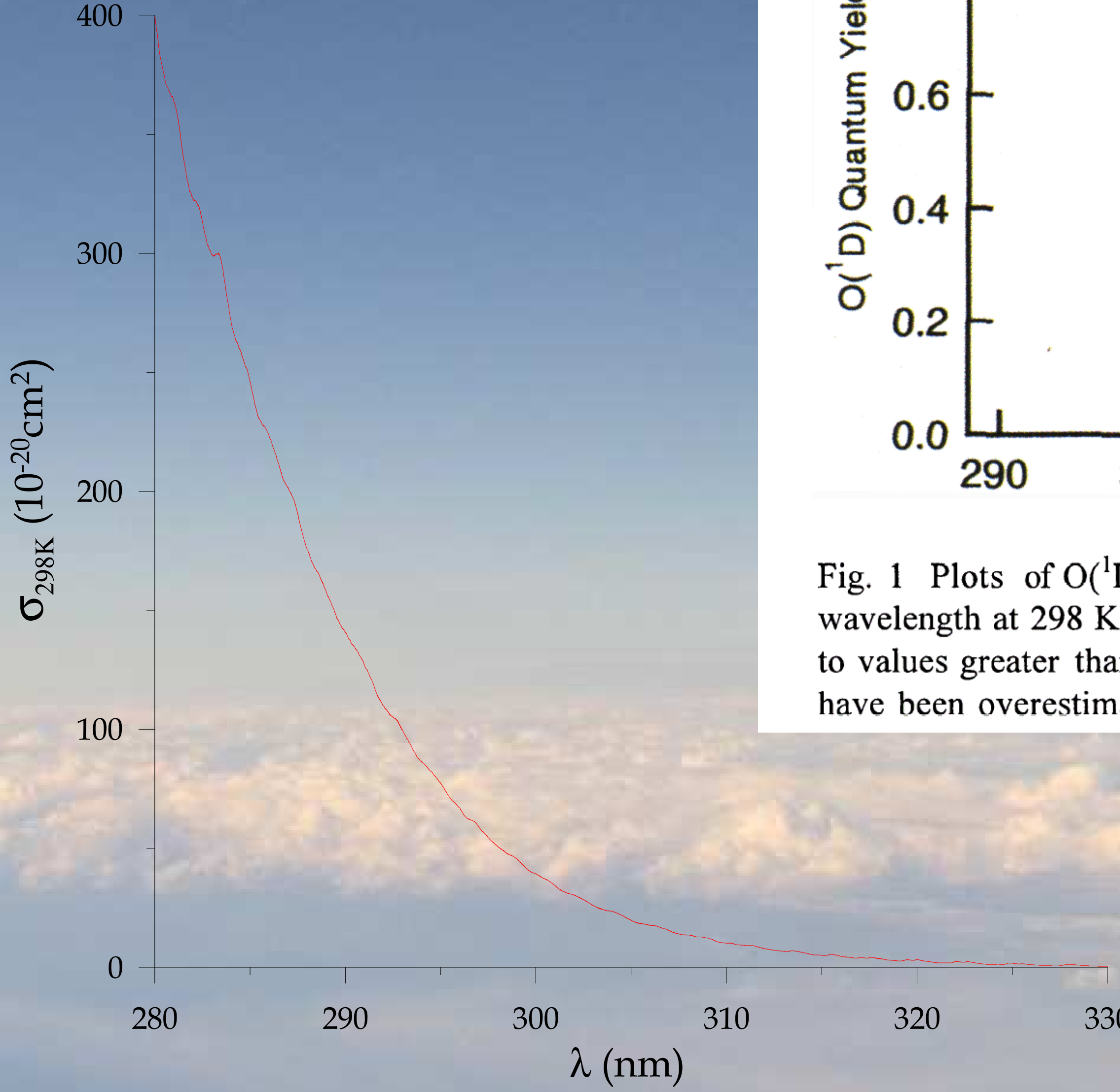

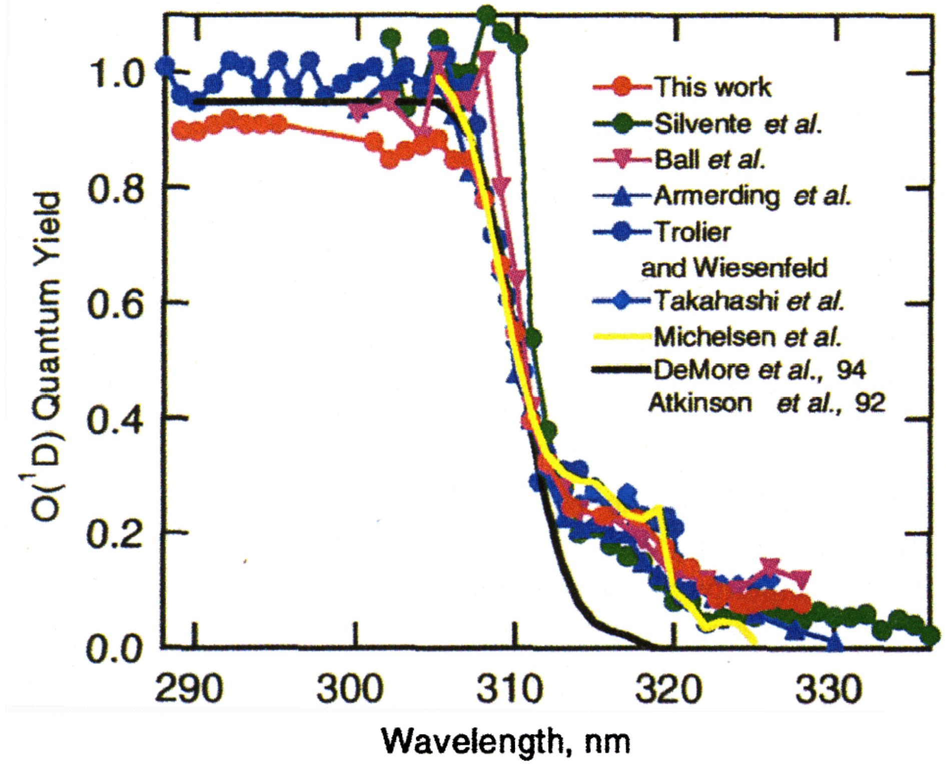

Fig. 1 Plots of O(^{1}D) quantum yield values as a function of wavelength at 298 K. Many of these studies were normalized to values greater than 0.89 at $\lambda < 305$ nm, and, therefore, may have been overestimated.

SPETTRORADIOMETRO METCON

Dimensioni	250 X 150 X100 mm^3
Peso	4.5 kg
Ingresso ottico	Cupola al quarzo, risposta angolare uniforme
Reticolo	248 linee mm^{-1}
Intervallo spettrale	280-700 nm
Rivelatore	*Array* di diodi con 512 elementi, 16 bit
Distanza spettrale	Circa 0.83 nm
Risoluzione (FWHM)	Circa 3 nm a 300 nm

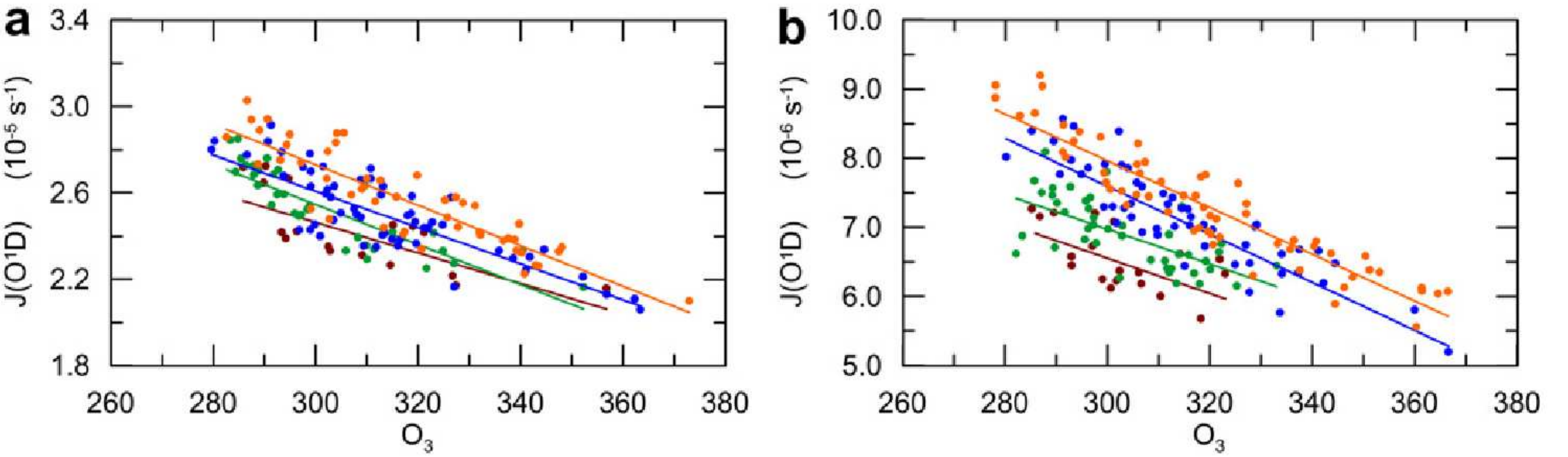

a
3.4
3.0
2.6
2.2
1.8
J(O1D) (10-5 s-1)
260
280
300
320
340
360
380
O3
b
10.0
9.0
8.0
7.0
6.0
5.0
J(O1D) (10-6 s-1)
260
280
300
320
340
360
380
O3

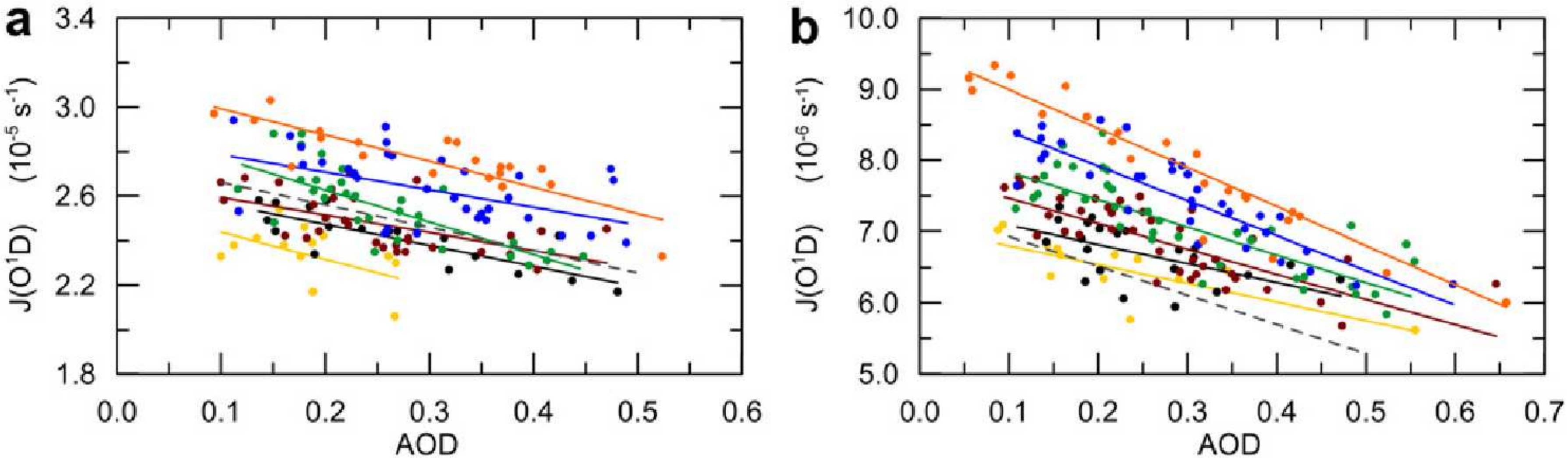
a
3.4
3.0
2.6
2.2
1.8
J(O¹D) (10⁻⁵ s⁻¹)
0.0
0.1
0.2
0.3
0.4
0.5
0.6
AOD
b
10.0
9.0
8.0
7.0
6.0
5.0
J(O¹D) (10⁻⁶ s⁻¹)
0.0
0.1
0.2
0.3
0.4
0.5
0.6
0.7
AOD

Lidar backscatter ratio

JULY 14 2002

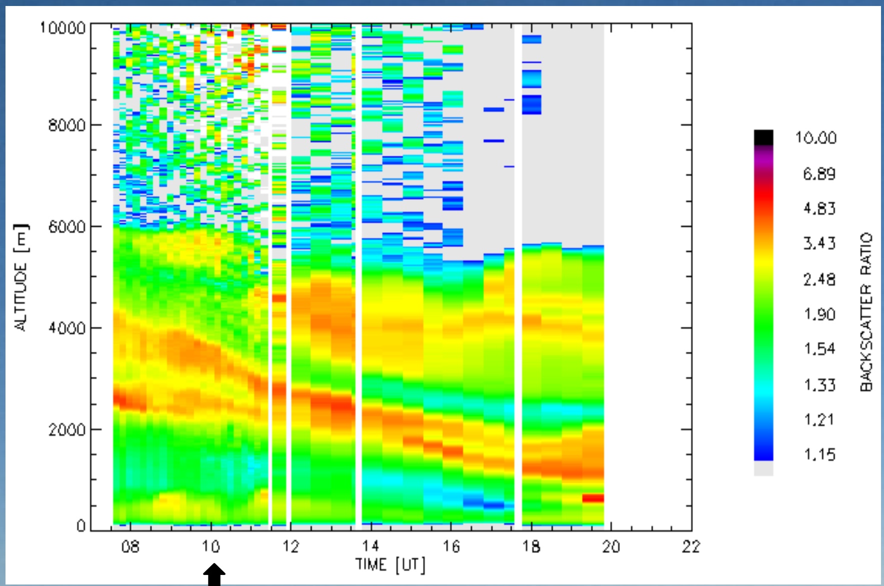

JULY 16 2002

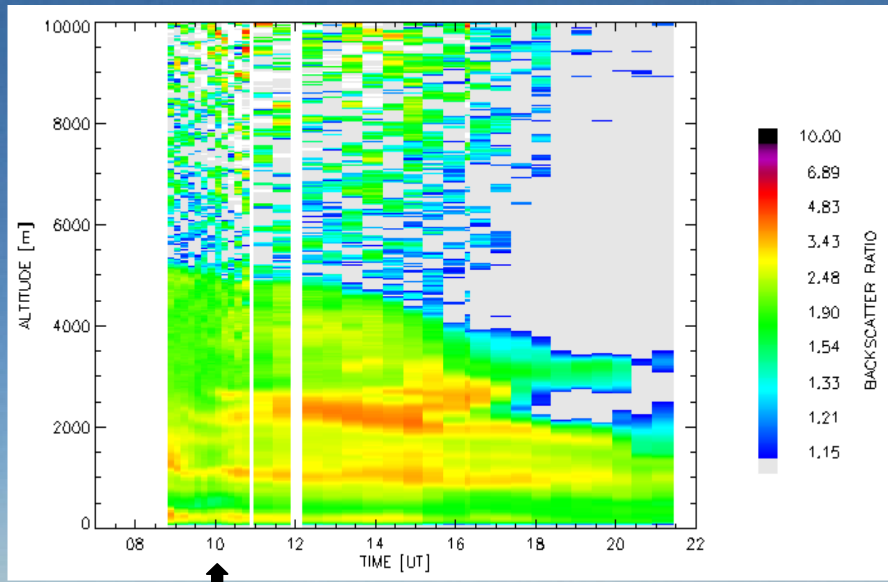

HYSPLIT transport and dispersion model from the NOAA Air Resources Laboratory (ARL)

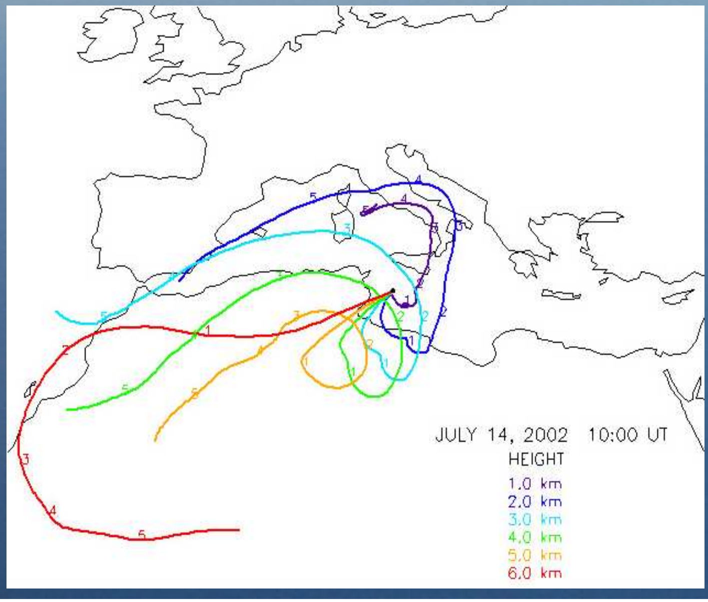

AOD (500 nm) = 0.227

14 July
α = 0.080
δ = 0.46-0.56

16 July
α = 0.698
δ = 0.25-0.47

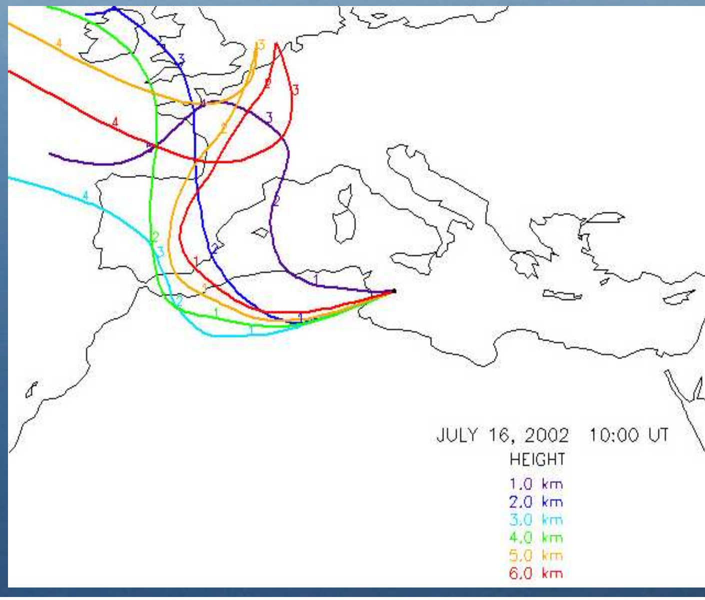

MISR (Multi-angle Imaging SpectroRadiometer)

on Terra spacecraft

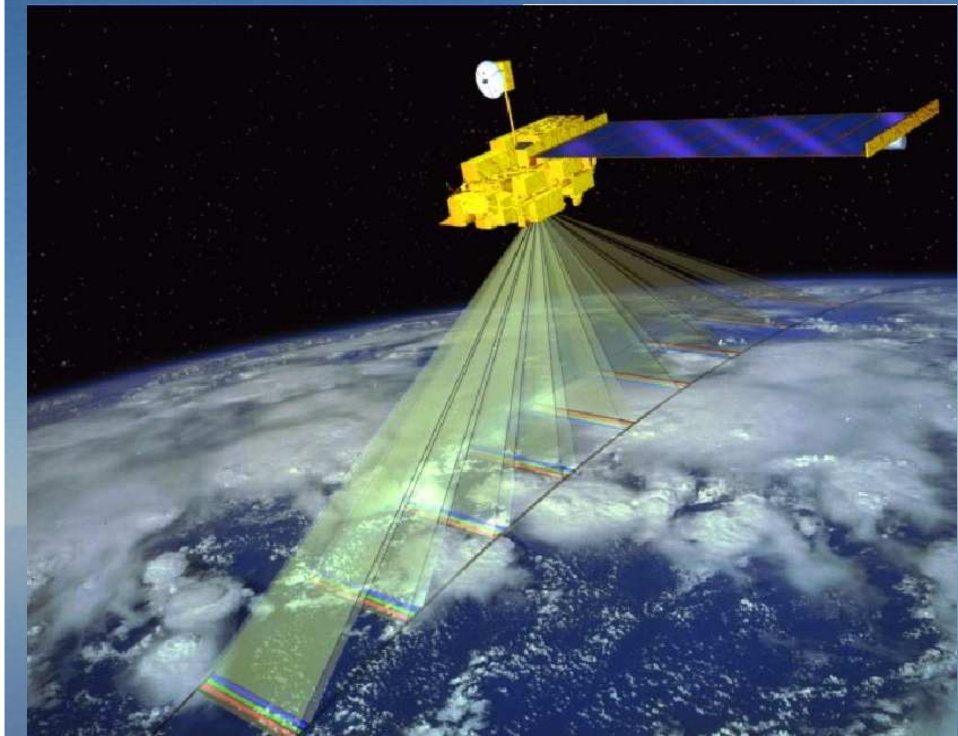

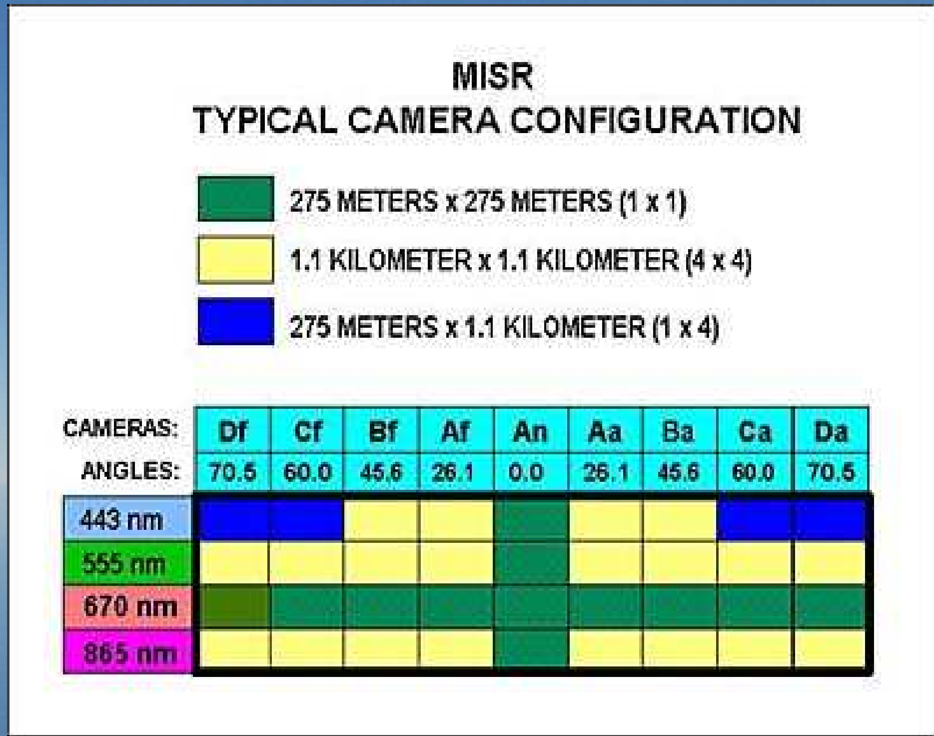

RESULTS

Best match (minimum RMDS) wavelength-independent SSA and *g*

14 July	16 July
SSA = 0.97 *g* = 0.80	**SSA = 0.88 *g* = 0.81**

Simulation of the MISR spectral (blue, red, green) equivalent reflectances at the nine viewing angles and comparison with measurements over the sea

$$\rho(i,k) = L(i,k) \times \pi \times d^2 / E_0(i)$$

i = band
k = camera

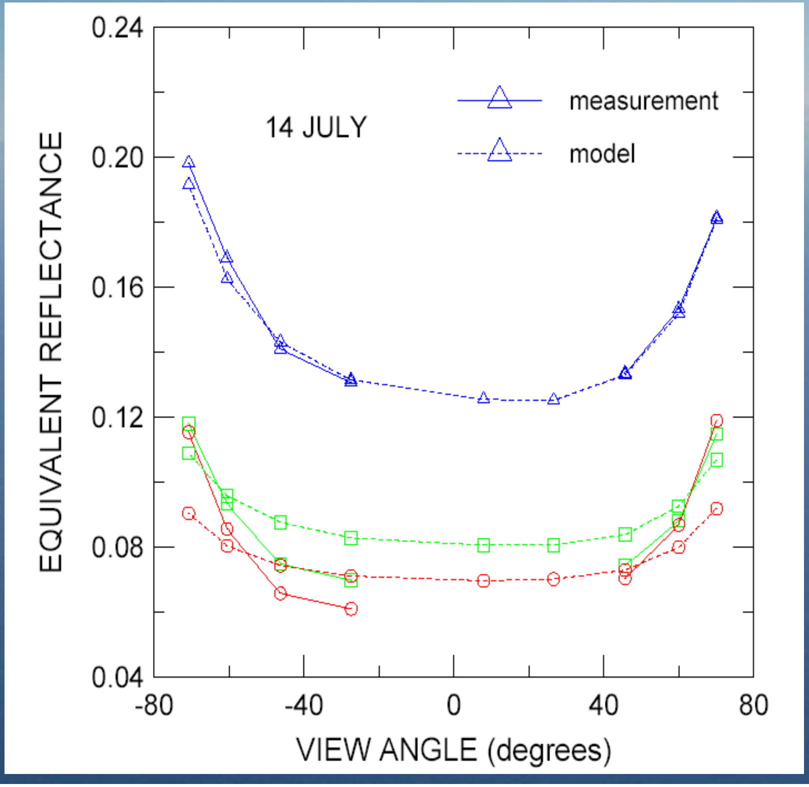

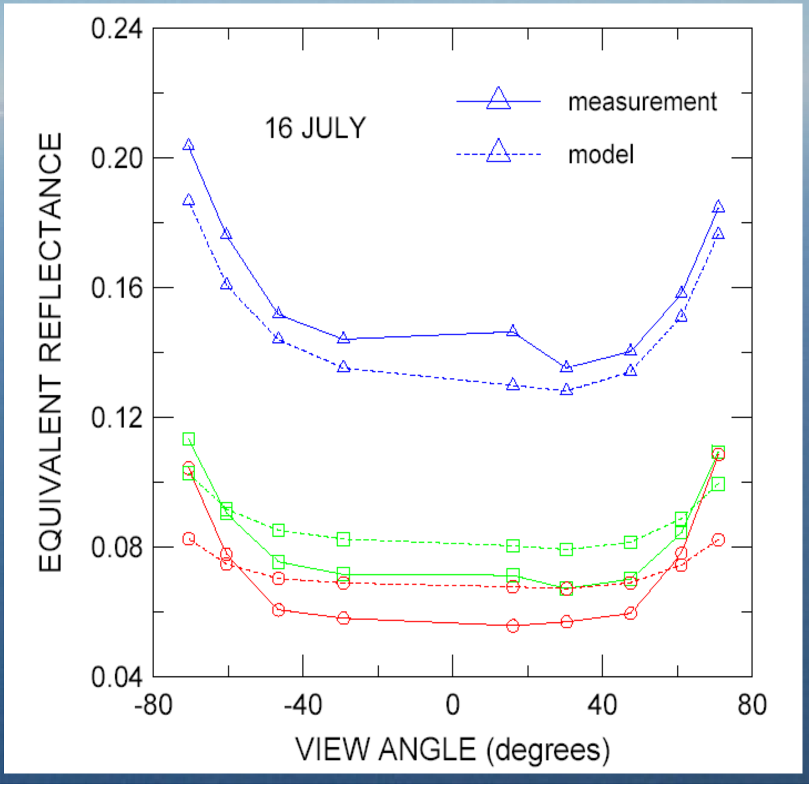

INSTANTANEOUS AEROSOL RADIATIVE FORCING EFFICIENCY

(RF per unit AOD at 500 nm)

AT 400-700 nm

RF (*surface*) = downward irr. $_{\text{(aerosol)}}$ - downward irr. $_{\text{(no aerosol)}}$

RF (TOA) = upward irr. $_{\text{(no aerosol)}}$ - upward irr. $_{\text{(aerosol)}}$

			Instantaneous RFE (W m^{-2})	
Day	ω_0	g	surface	TOA
14/07/2002	0.96	0.79	-39.3	-17.3
	0.97	0.80	-44.2	-20.1
16/07/2002	0.88	0.81	-73.2	-5.1
	0.89	0.82	-79.0	-7.4